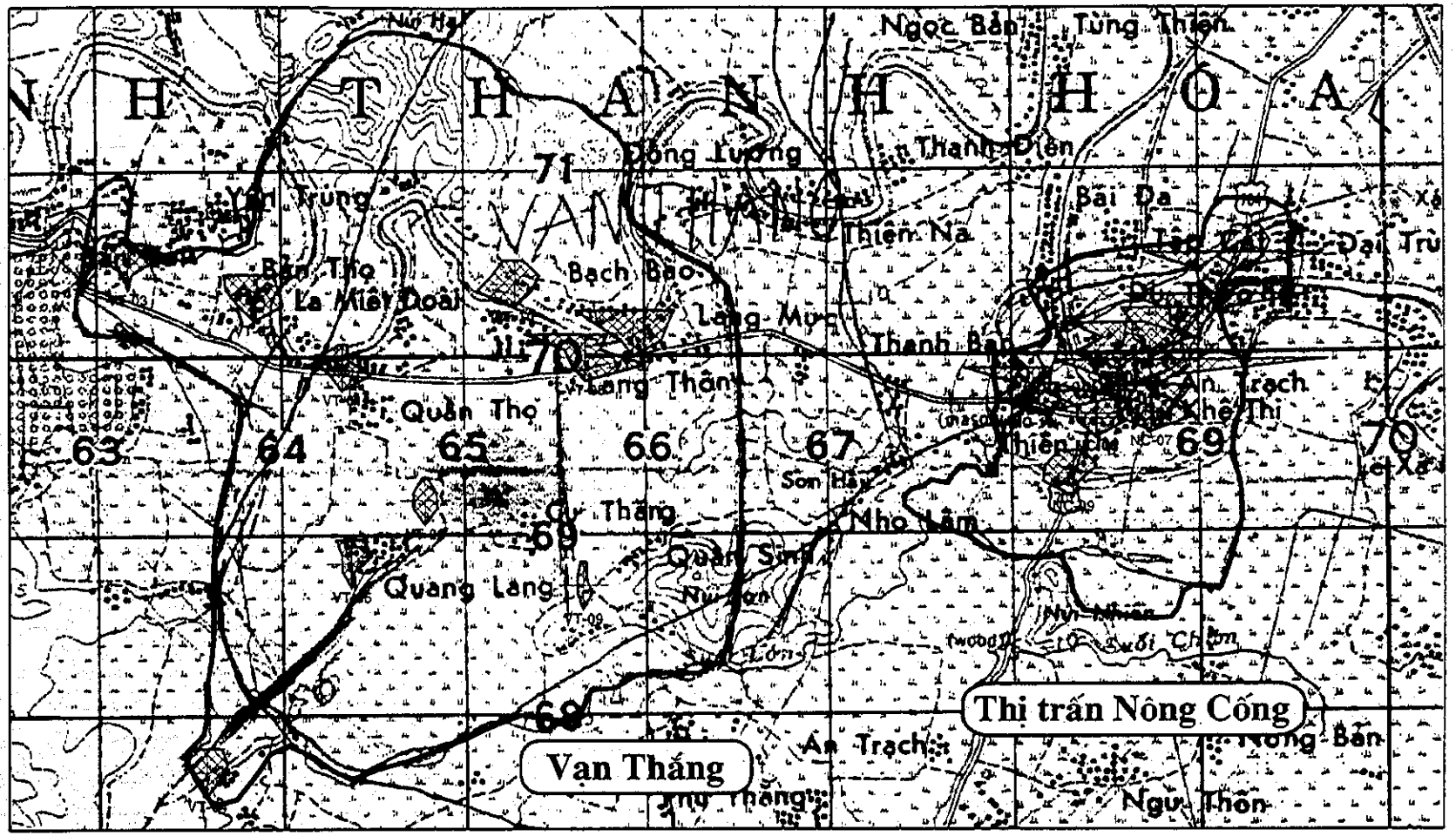

Figure 1.33	Stiff Diagram of Thị trấn Nông Cống and Vạn Thắng Communes, Thanh Hóa Province
THE STUDY ON GROUNDWATER DEVELOPMENT IN THE RURAL PROVINCES OF NORTHERN PART IN THE SOCIALIST REPUBLIC OF VIETNAM	
JAPAN INTERNATIONAL COOPERATION AGENCY (JICA)	

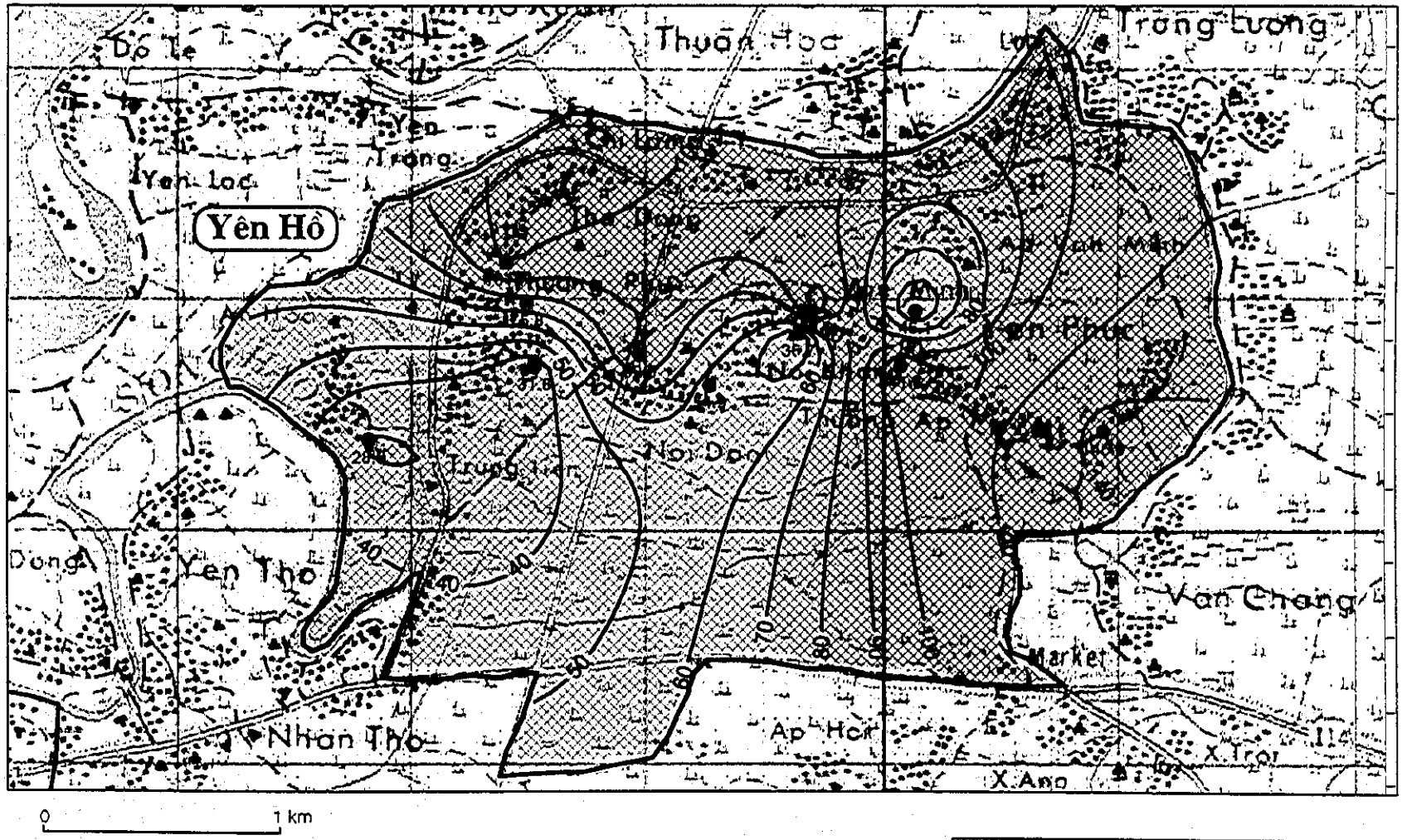

Figure 1.34	Distribution of EC values in Yên Hồ Commune, Hà Tĩnh Province

THE STUDY ON GROUNDWATER DEVELOPMENT IN THE RURAL PROVINCES OF NORTHERN PART IN THE SOCIALIST REPUBLIC OF VIETNAM

JAPAN INTERNATIONAL COOPERATION AGENCY (JICA)

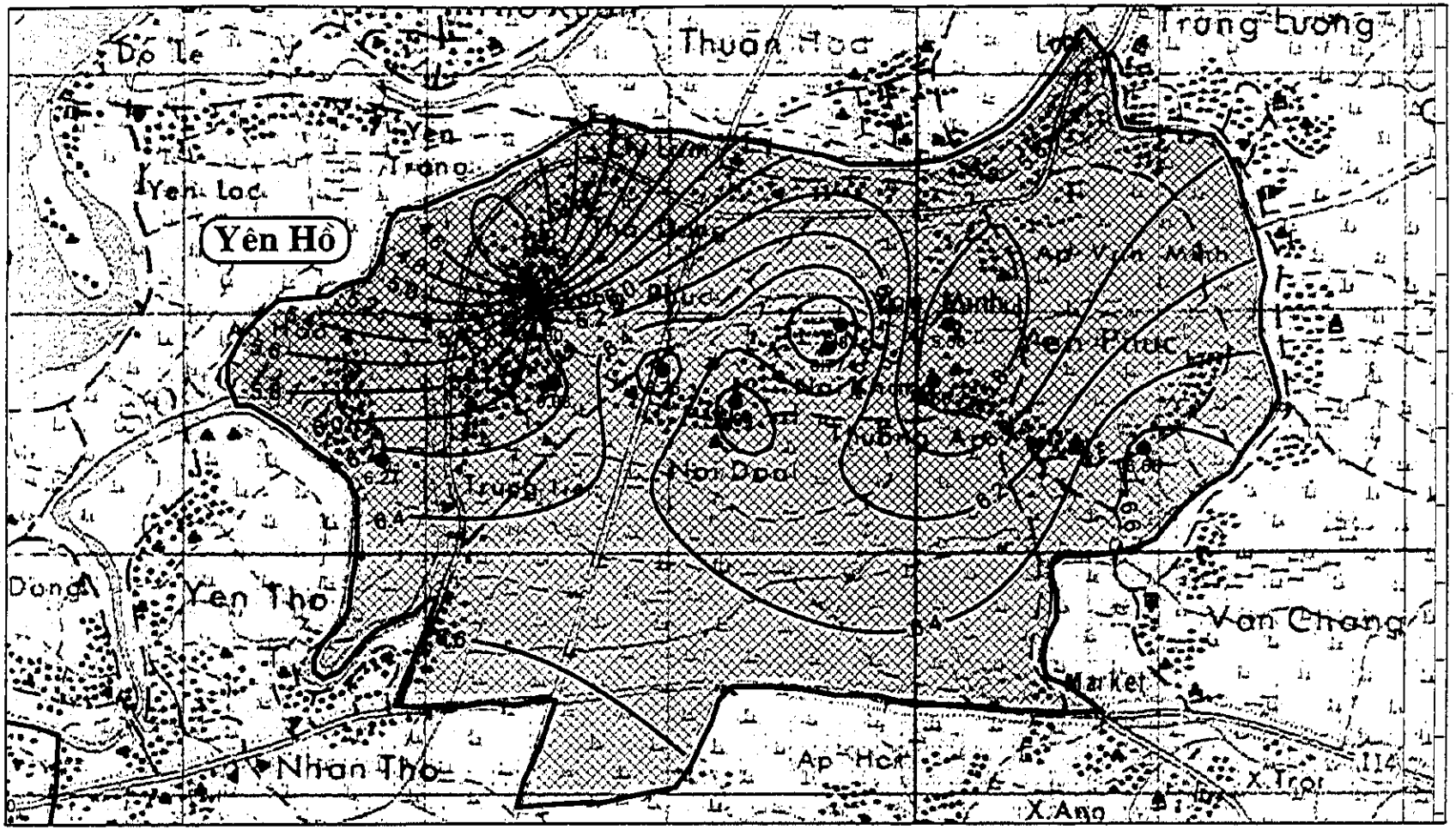

Figure 1.35	Distribution of pH values in Yên Hồ Commune, Hà Tĩnh Province

THE STUDY ON GROUNDWATER DEVELOPMENT IN THE RURAL PROVINCES OF NORTHERN PART IN THE SOCIALIST REPUBLIC OF VIETNAM

JAPAN INTERNATIONAL COOPERATION AGENCY (JICA)

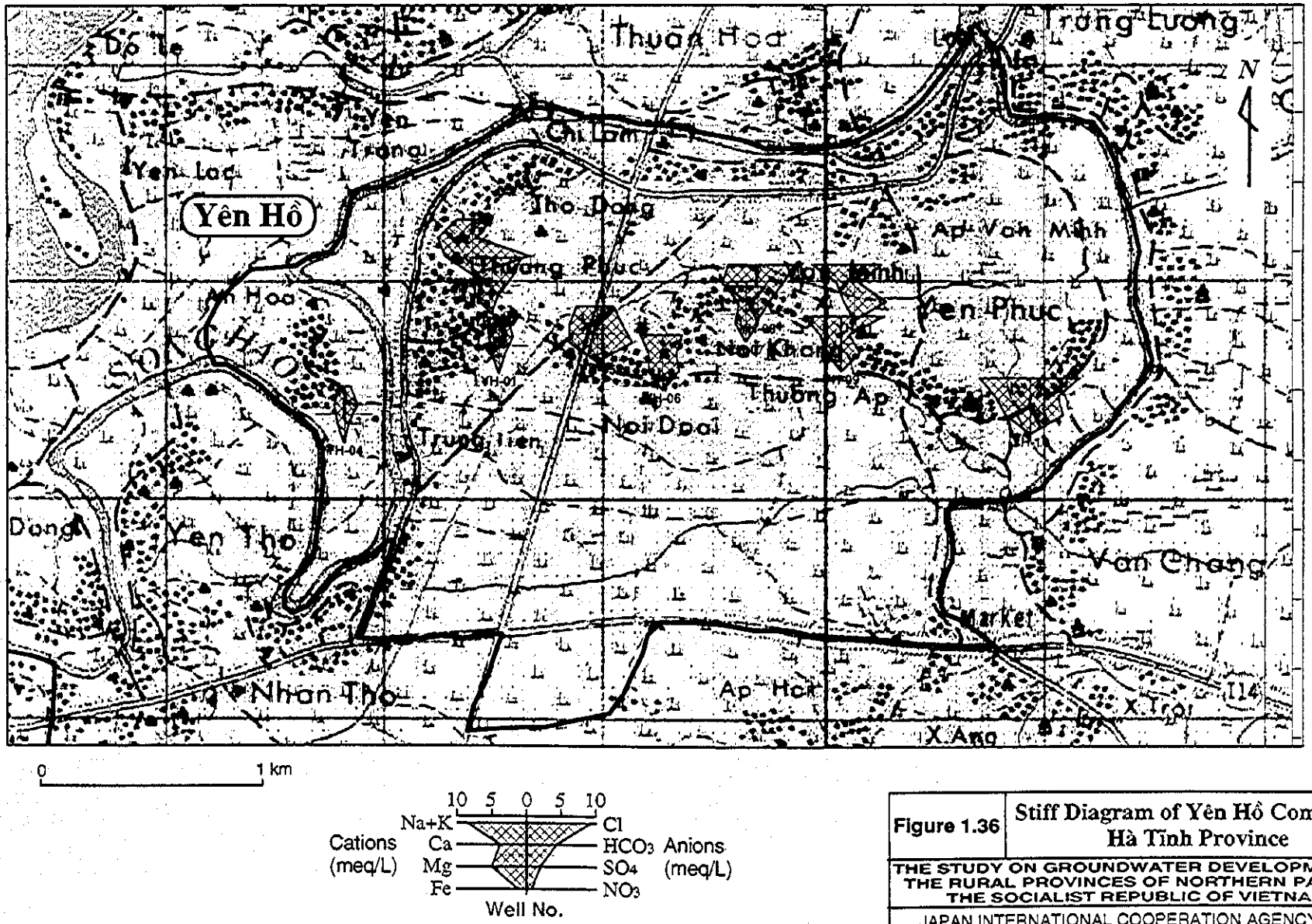

Figure 1.36	Stiff Diagram of Yên Hô Commune, Hà Tĩnh Province

THE STUDY ON GROUNDWATER DEVELOPMENT IN THE RURAL PROVINCES OF NORTHERN PART IN THE SOCIALIST REPUBLIC OF VIETNAM

JAPAN INTERNATIONAL COOPERATION AGENCY (JICA)

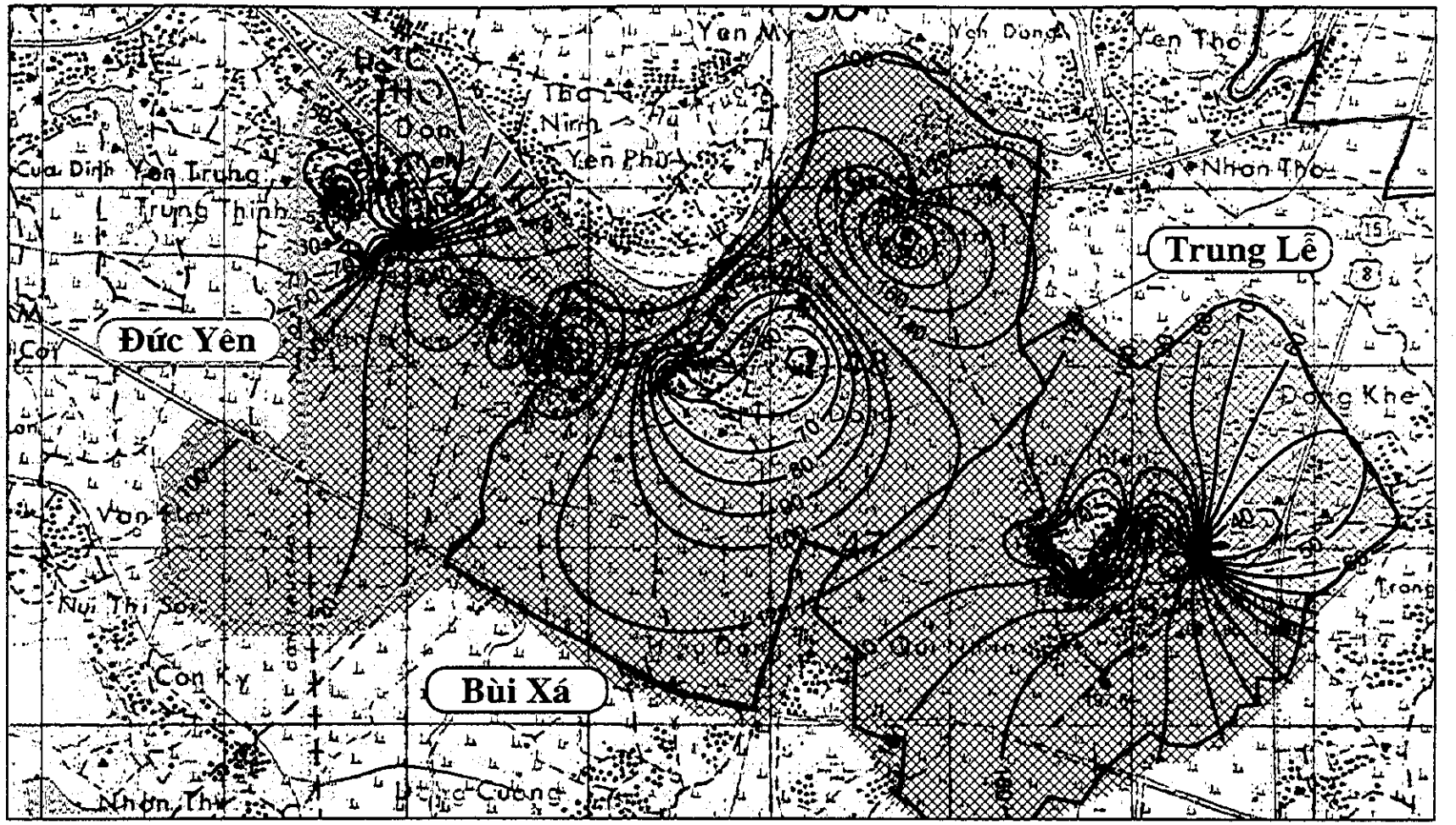

Figure 1.37	Distribution of EC values in Đức Yên, Bùi Xá and Trung Lễ Communes, Hà Tĩnh Province

THE STUDY ON GROUNDWATER DEVELOPMENT IN THE RURAL PROVINCES OF NORTHERN PART IN THE SOCIALIST REPUBLIC OF VIETNAM

JAPAN INTERNATIONAL COOPERATION AGENCY (JICA)

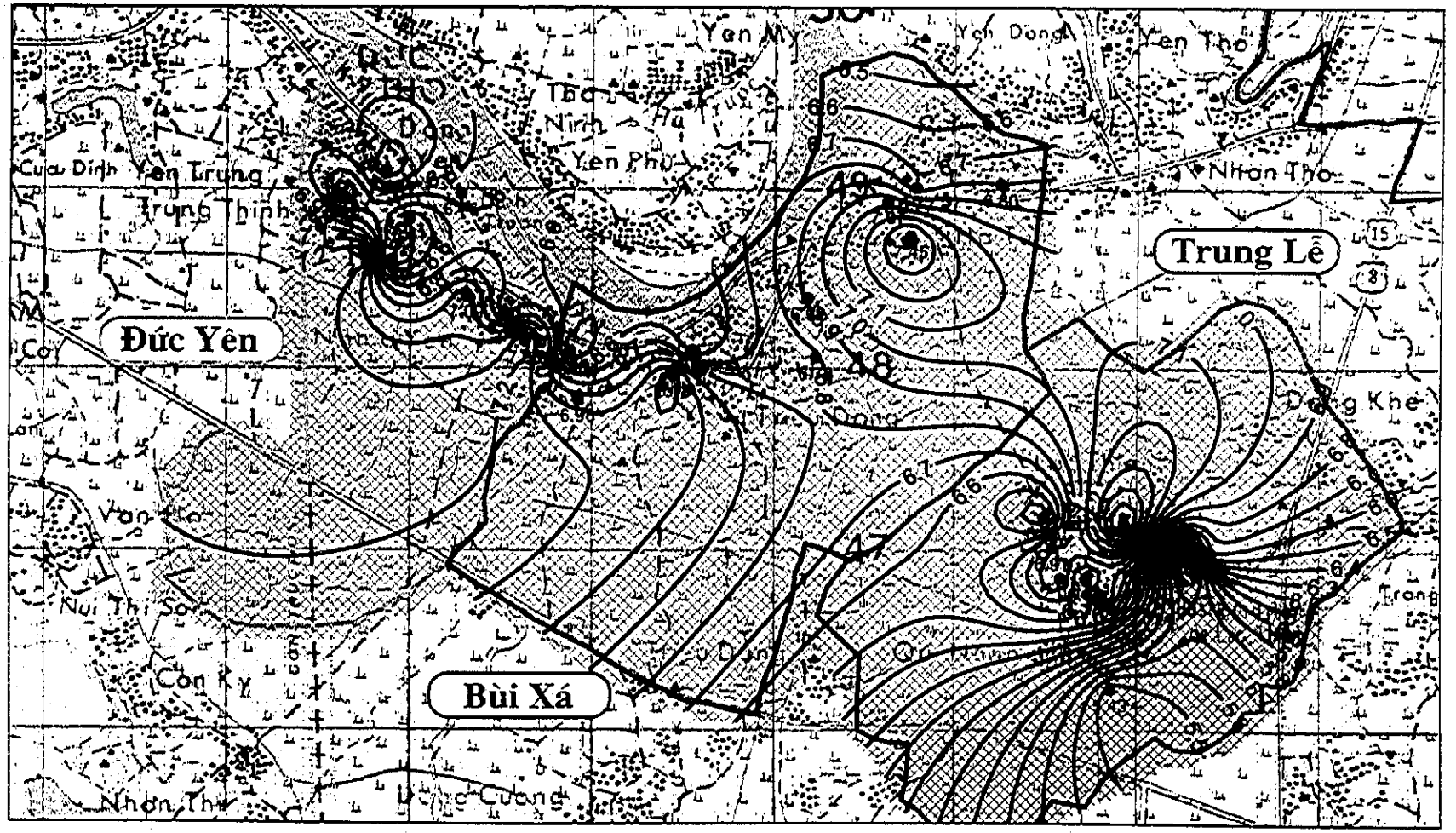

Figure 1.38	Distribution of pH values in Đức Yên, Bùi Xá and Trung Lễ Communes, Hà Tĩnh Province

THE STUDY ON GROUNDWATER DEVELOPMENT IN THE RURAL PROVINCES OF NORTHERN PART IN THE SOCIALIST REPUBLIC OF VIETNAM

JAPAN INTERNATIONAL COOPERATION AGENCY (JICA)

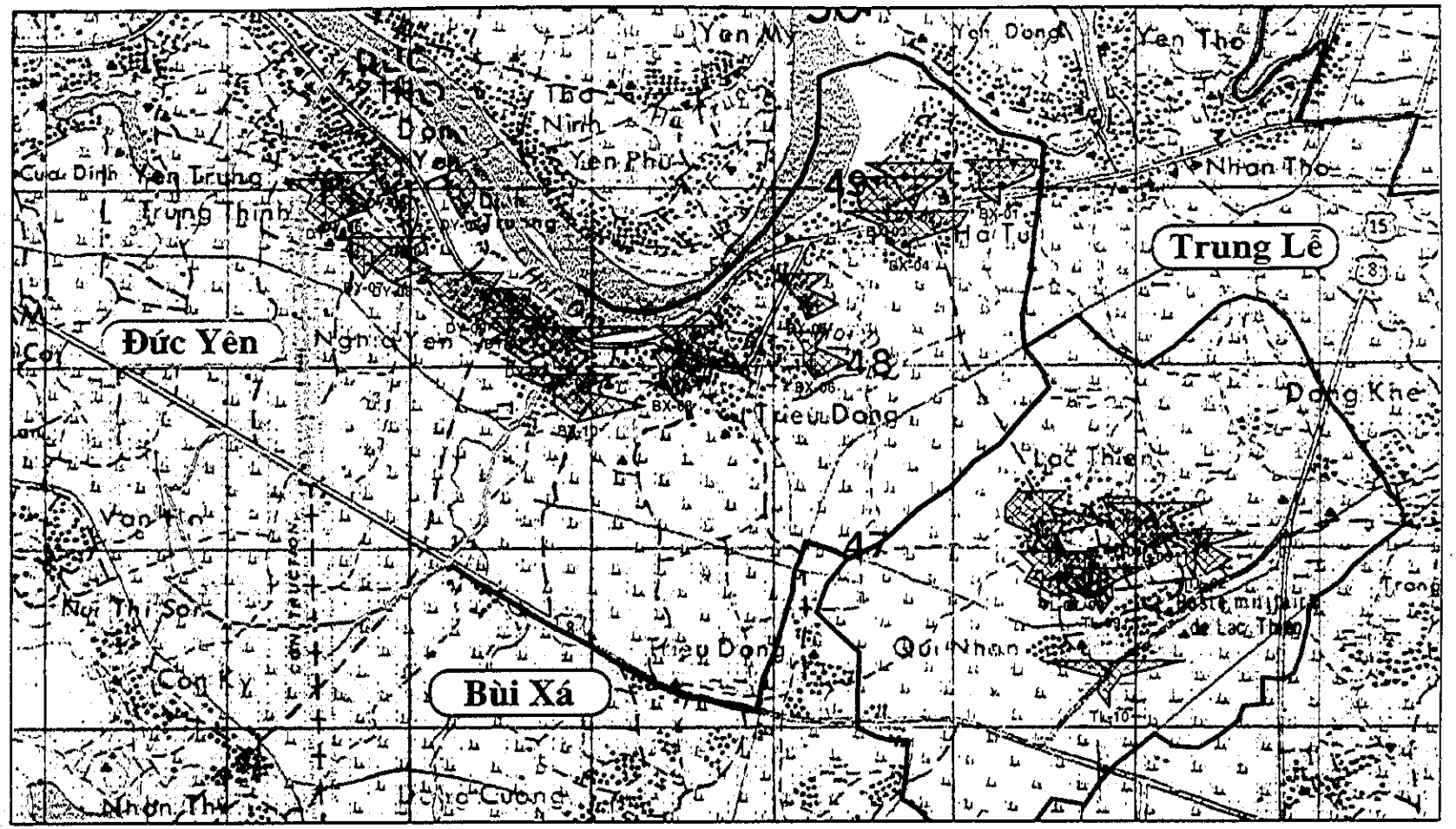

Figure 1.39	Stiff Diagram of Đức Yên, Bùi Xá and Trung Lễ Communes, Hà Tĩnh Province

THE STUDY ON GROUNDWATER DEVELOPMENT IN THE RURAL PROVINCES OF NORTHERN PART IN THE SOCIALIST REPUBLIC OF VIETNAM

JAPAN INTERNATIONAL COOPERATION AGENCY (JICA)

CHAPTER 2

GEOPHYSICAL PROSPECTING

CHAPTER 2 GEOPHYSICAL PROSPECTING

2.1 Principle and Interpretation

2.1.1 VES Method

(1) Principle

Vertical Electric Survey (VES) is one-dimensional electric prospecting. What electrical boundaries and resistivity of underground will be obtained with simple measurement and analysis mark this method. Therefore, Vertical electric prospecting can be applied in case that underground has an approximately horizontally layered structure. Electric potentials are measured by the Schlumberger Electrode array shown in Figure 2.1.

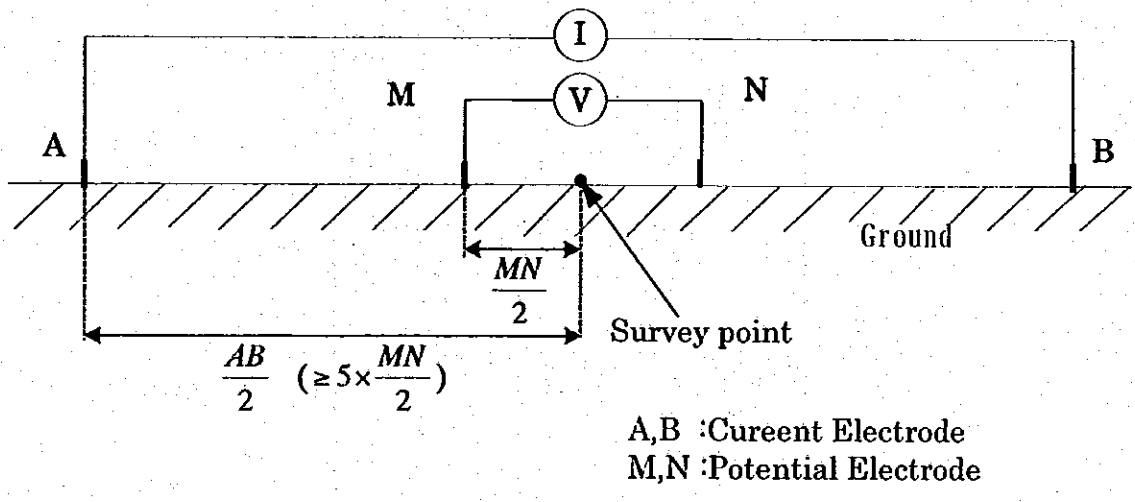

Figure 2.1 Schematic diagram of Schlumberger Electrode array

(2) Field Measurement

At first, two pairs of electrodes, which are current electrodes (A, B) and potential ones (M, N), set on the ground making measurement point into center, shown in Figure 2.2. The current electrode injects a current into the ground, and the potential electrode measures the electric potential.

Next, pair of electrodes spread making measurement point into center. The distance between A and B are maintained at least five times than the distance between M and N (See Table 2.1).

Table 2.1 The measurement schedule of Schlumberger Electrode array

AB/2 (m)	MN/2 (m)	K
1.5	0.5	6.28
2.5	0.5	18.85
3.0	0.5	27.49
4.0	0.5	49.48
5.0	0.5	77.75
6.0	0.5	112.31
7.0	0.5	153.15
8.0	0.5	200.28
8.0	3.0	28.80
10.0	0.5	313.37
10.0	3.0	47.65
13.0	3.0	83.78
17.0	3.0	146.61
20.0	3.0	204.73
25.0	3.0	322.54
30.0	3.0	466.53
40.0	3.0	833.05
50.0	3.0	1,304.28
60.0	3.0	1,880.24
80.0	3.0	3,346.32
80.0	20.0	471.24
100.0	3.0	5,231.28
100.0	20.0	753.98
130.0	20.0	1,295.91
170.0	20.0	2,238.38
200.0	20.0	3,110.18

The more current electrode spread, the deeper electric potential can be obtained. In this prospecting, we have AB/2: 200 meters maximum.

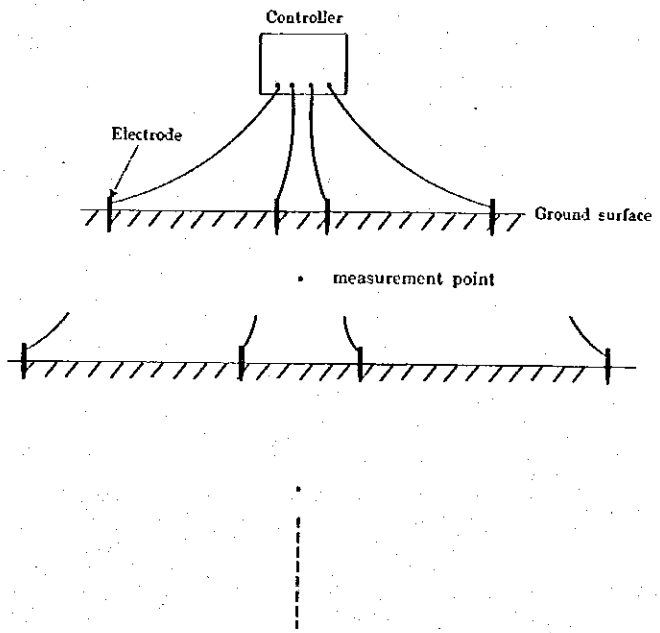

Figure 2.2 Schematic diagram of field measurement and measurement process.

(3) Analysis

The flow chart of the automatic inversion is shown in Figure 2.3. This is based on an iterative method.

First, an apparent resistivity pseudo-section is calculated from the corrected data by following equation.

$$\rho_a = \pi \frac{AB^2 - MN^2}{4MN} \frac{V}{I}, AB \geq 5MN$$

This pseudo-section is usually used as the initial model for the inversion. If the pseudo-section does not produce adequate convergence, an average model is used for the initial model.

Next, theoretical potential data corresponding to the model are computed. Alternatively, if the underground has an approximately horizontally layered structure, the digital linear filter method (Ghosh, 1971a, b) can be used to conduct continuous one-dimensional inversion. After theoretical potential data are calculated, the model is modified to reduce the residuals between the theoretical data and the measured data. To find the model giving the minimum residuals, the non-linear least squares technique is

applied. This modification process is iterated until the residuals become sufficiently small or subsequent changes to the model no longer improve the fitting. At this point, the inversion is considered to have converged.

The final, resistivity model is displayed as a color profile that clearly shows the resistivity structure.

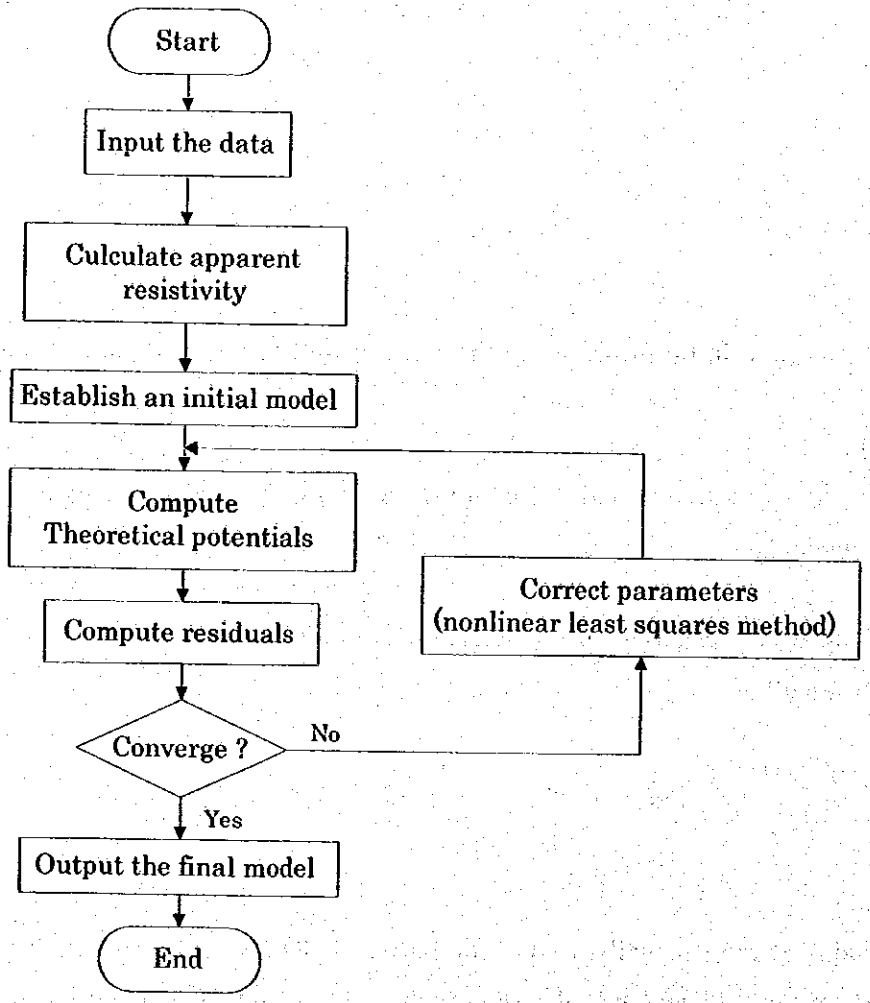

Figure 2.3 Flow chart of automatic inversion

2.1.2 RIP Method

(1) Principle

Horizontal Electric Prospecting is one of the electric prospecting that noticing proper ground resistivity. The Resistivity Image Profiling (RIP) uses inversion techniques to analyze a two-dimensional resistivity distribution and displays the results as a colored profile. These analysis results show a more detailed and reliable resistivity distribution than VES. Electric potentials are measured by the pole-pole electrode array shown in Figure 2.4.

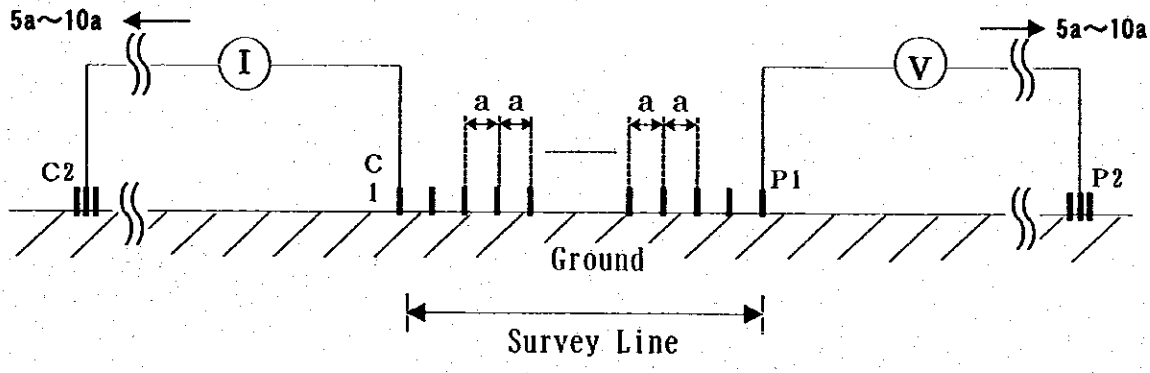

C1:Cureent Electrode (moving)
C2:Cureent Electrode (remote)
P1:Potential Electrode (moving)
P2:Potential Electrode (remote)

Figure 2.4 Schematic diagram of pole-pole electrode array

In general, the relation between resistance R (ς) and resistivity ρ (ς m) obtained by pole-pole array is expressed as equation (1):

$$R = \rho \cdot \frac{l}{S} \qquad \cdots (1)$$

And electric potential V (volt) by Ohm's low is:

$$V = R \cdot I = \rho \cdot \frac{l}{S} \cdot I \qquad \cdots (2)$$

where l is length, S is the area section, I (ampere) is the intensity of the injected current.

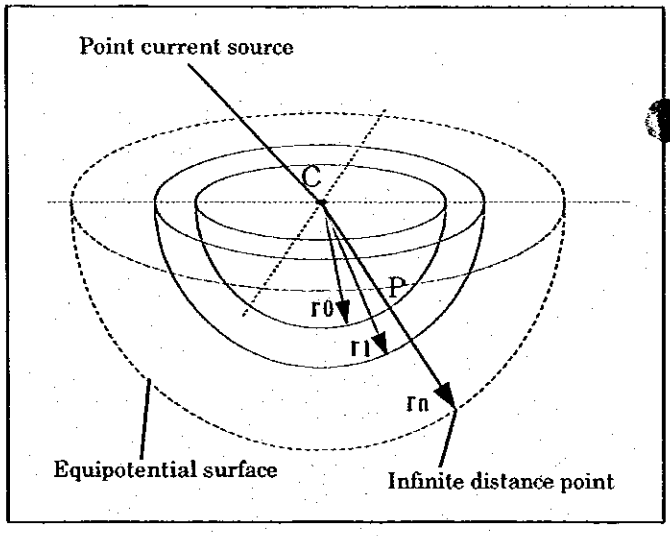

Figure 2.5 Potential distribution with point current source

In hemisphere in flat ground (see Figure 2.5), electric potential difference $V_{r_0-r_1}$ between radius r_0 and r_1 is obtained as:

$$V_{r0-r1} = \rho \cdot \frac{l}{S} \cdot I \qquad \cdots (3)$$

Surface area of hemisphere S is:

$$S = \frac{4\pi r^2}{2} = 2\pi r^2 \qquad \cdots (4)$$

If $r_0 \cong r_1$, then e.q. (4) gives:

$$S = 2\pi r^2 = 2\pi r_0 r_1 \qquad \cdots (4)'$$

Since $l = r_1 - r_0$, e.q. (3) is written as:

$$V_{r_0-r_1} = \rho \cdot \frac{r_1 - r_0}{2\pi r_0 \cdot r_1} \cdot I = \frac{\rho I}{2\pi} \cdot \left(\frac{1}{r_0} - \frac{1}{r_1}\right) \qquad \cdots (5)$$

Electric potential at P is obtained the sum of electric potential difference from equipotential surface at radius r_n to r_0.

$$\begin{aligned} V_P &= V_{r_0-r_1} + V_{r_2-r_2} + \cdots + V_{r_0-r_1-r_n} \\ &= \frac{\rho I}{2\pi} \cdot \left(\frac{1}{r_0} - \frac{1}{r_1} + \frac{1}{r_1} - \frac{1}{r_2} + \cdots + \frac{1}{r_{n-1}} - \frac{1}{r_n} \right) \quad \cdots (6) \\ &= \frac{\rho I}{2\pi} \cdot \left(\frac{1}{r_0} - \frac{1}{r_n} \right) \end{aligned}$$

r_n is defied as an infinite distance point from current point source (C). Thus e.q. (6) is given as:

$$V = \frac{\rho \cdot I}{2\pi} \cdot \frac{1}{r_0} \quad \cdots (7)$$

where $\frac{1}{r_n} = 0$.

In the case of homogeneous, resistivity ρ is given as:

$$\rho = 2\pi r \frac{V}{I} \quad \cdots (8)$$

(2) Field Measurement

Figure 2.6 shows that simple diagram of field measurement of pole-pole array. In this array, one electrode, C1, injects a current into the ground, and one electrode, P1, measures the electric potential. These two electrodes are called "moving electrodes". Another potential electrode, P2, is needed to provide a reference for the potential at P1. Electrodes C2 and P2 should be located very far from the moving electrode so that they have a negligible effect on the measurement. We call C2 and P2 "remote electrode". For actual measurement, the distance between a remote electrode and a moving electrode is maintained at least five times than the maximum distance between the moving electrodes.

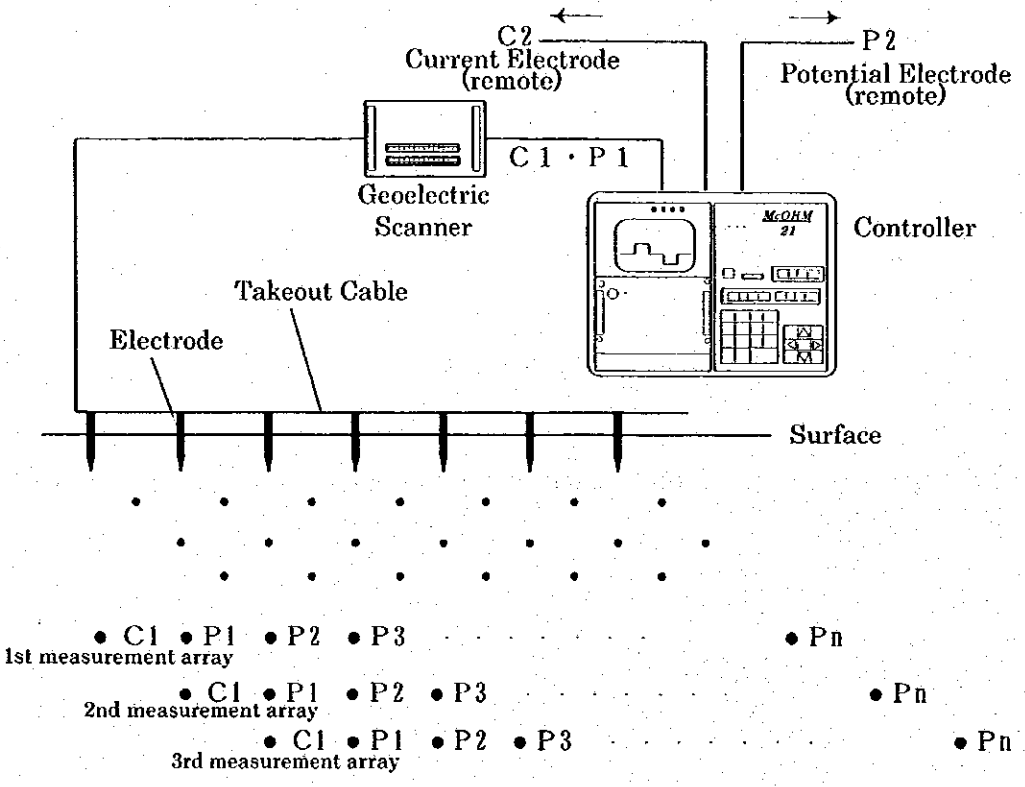

Figure 2.6 schematic diagram of field measurement and measurement process.

(3) Analysis

The flow chart of the automatic inversion is shown in Figure 2.7. This is based on an iterative method.

First, terrain effects are estimated using the finite element method (Coggon, 1971). These effects then are eliminated from the measured potential data. Next, an apparent resistivity pseudo-section is produced from the corrected data. This pseudo-section is usually used as the initial model for the inversion. If the pseudo-section does not produce adequate convergence, an average model is used for the initial model.

Next, theoretical potential data corresponding to the model are computed. Alternatively, if the underground has an approximately horizontally layered structure, the digital linear filter method (Ghosh, 1971a, b) can be used to conduct the Continuous one-dimensional inversion. After theoretical potential data are calculated, the model is modified to reduce the residuals between the theoretical data and the measured data. To find the model giving the minimum residuals, the non-linear least squares technique is applied. This modification process is iterated until the residuals become sufficiently

small or subsequent changes to the model no longer improve the fitting. At this point, the inversion is considered to have converged.

The final, resistivity model is displayed as a color profile that clearly shows the resistivity structure.

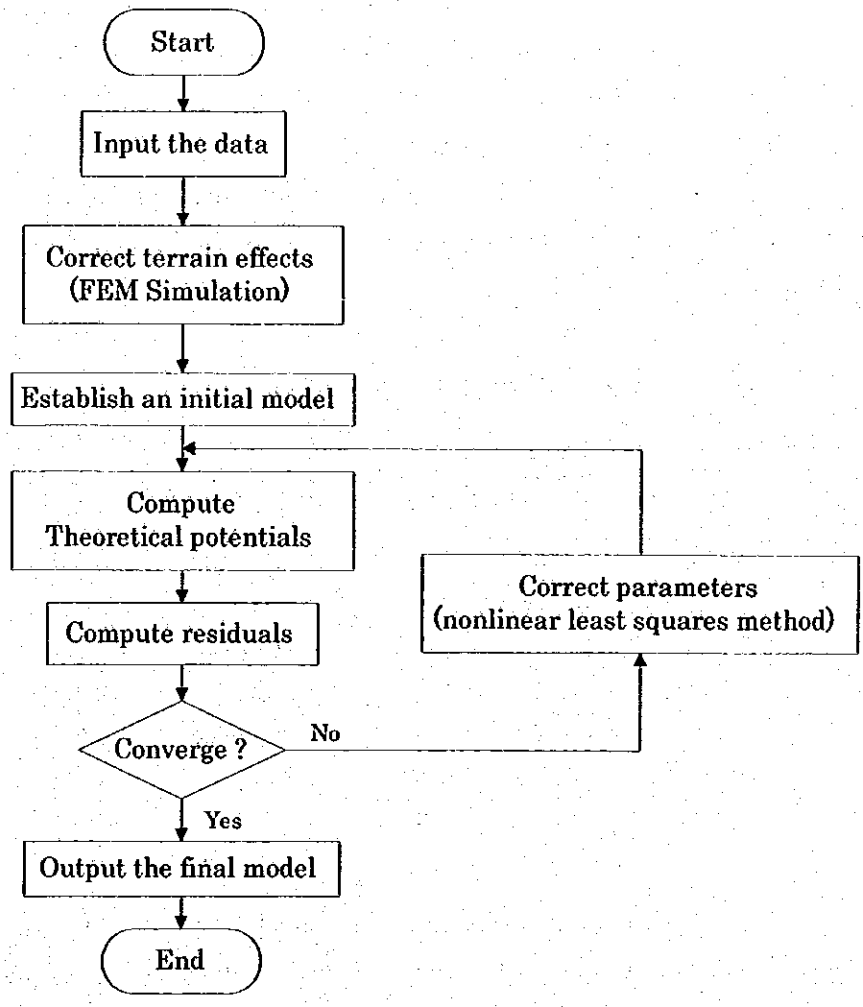

Figure 2.7 Flow chart of 2-D automatic inversion

2.1.3 VLF Method

(1) Principle and characteristic

The Very Low Frequency (VLF) method is an electromagnetic geophysical method that aims at detecting conductive or resistive zones located at depths of a few tens meters.

It uses the electromagnetic carrier waves produced by military transmitters in order to communicate with submarines (Table 2.2: location of the major transmitters). These waves —called primary fields in the VLF method— have a frequency of 15 to 30 kHz and are propagated between the surface of the earth and the ionosphere. In the presence of conductive bodies, the primary field induces secondary currents inside, and these currents generate a secondary field. Thus, the measurement of the total field (primary1secondary) at the surface of the earth can help in detecting conductive structures located in the prospective area.

Table 2.2 Major Transmitter

Call sign	Place	Frequency	Call sign	Place	Frequency
FUO(1)	France	15.1kHz	NSS	U.S.A	21.4kHz
FUO(2)	India	15.1kHz	GBZ	England	19.6kHz
GBR	England	16.0kHz	ICV	Italy	20.27kHz
FUB	French	16.8kHz	NWC	Australia	22.3kHz
UMS	Moscow	17.1kHz	NPM	Hawai	23.4kHz
JJT	Japan	22.2kHz	LPZ	Argentino	23.6kHz
HN	Norway	17.6kHz	NBA	Panama	24.0kHz
NAA	U.S.A	24.0kHz	NLK	U.S.A	27.5kHz

One major benefit of VLF methods is that a personal transmitter is not needed to produce the primary electromagnetic wave, which can save time and reduces exploration costs. However, one must keep in mind that these transmitters sometimes stop transmitting for maintenance. Besides, the level of the signal which are measured can be low during some hours in the day depending on the propagation conditions and on the distance between the transmitting antenna and the prospected area.

In spite of these drawbacks, the VLF method is widely used for prospecting shallow conductive or sometimes resistive geological formations. It is a valuable help to geology mapping.

(2) Depth of Investigation

The depth of investigation of the methods on the one hand on the shape and dimensions of the anomalous bodies, and on the other hand on the resistivity of the host medium and of that of the anomalous bodies. The frequency of the transmitters being fixed, vertical soundings can not be performed with such a method.

No absolute rule can be given, but in a first approximation, the depth of investigation of VLF methods can be estimated in the order of 50 m for a 1,000 ohm-m resistivity host medium, 20 m for 100 ohm-m and 5 m for 10 ohm-m.

(3) Tilt and Ellipticity

The magnetic field which has horizontal and vertical components describes an ellipse that can be characterized by the tilt angle of its major axis from horizontal, and its ellipticity (ratio of the minor axis to the major axis). These two parameters can be calculated from the measurements of the in-phase and out-of-phase (quadrature) components of the vertical magnetic field with respect to the horizontal one.

Figure 2.8 shows the tilt angle anomaly observed along a profile crossing a vertical conductive dyke. It can be seen that a maximum and a minimum tilt angle separated by an inflexion point located above the top of the dyke.

In case of the applying highly conductive structures, the ellipticity value is less than the tilt value and has an opposite sign. In poorly conductive structures or geological contacts, the ellipticity value is of the same order as the tilt value and has the same sign.

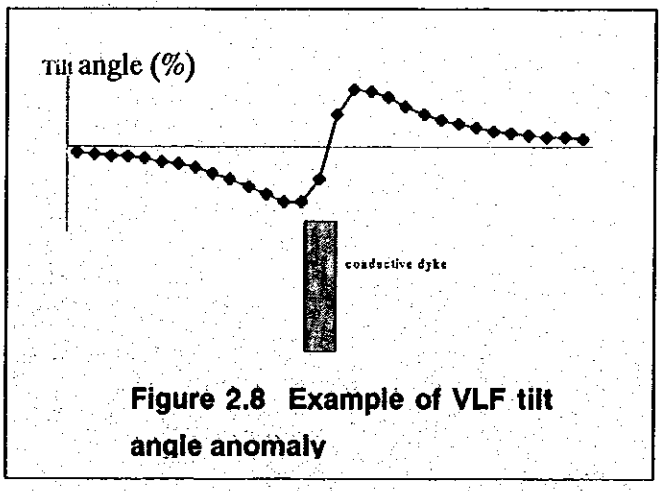

Figure 2.8 Example of VLF tilt angle anomaly

2.2 Results

2.2.1 VES Method

The interpretation results of VES are presented in the Main Report. The result of each VES survey is presented the Data Report.

2.2.2 RIP Method

Figures 2.9 to 2.31 show the results of RIP. The profile of resistivity distribution up to a depth of 150 m along the survey line is presented.

2.2.3 VLF Method

Figures 2.24 to 2.41 show the results of VLF. At each survey line, the tilt angle and ellipticity were show. If a power line intersects the survey line, the location of the power line is indicated on the graph. Because the existence of power line affects the result of VLF measurement.

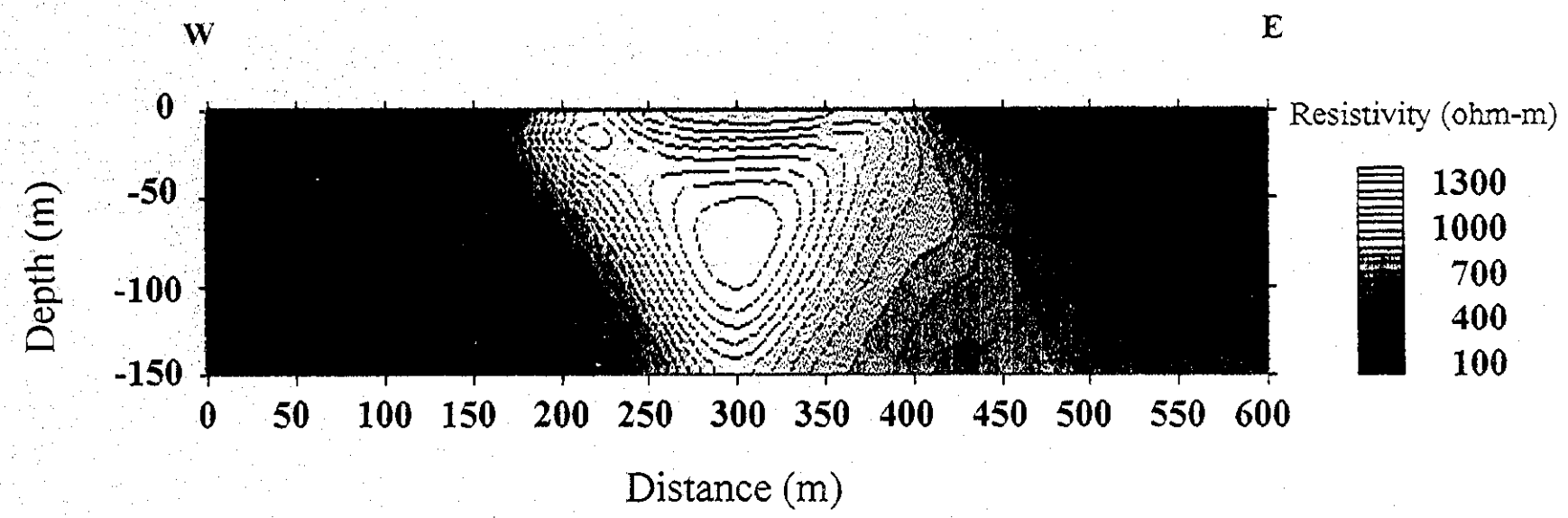

Figure 2.9 RIP result -Hóa Thương-

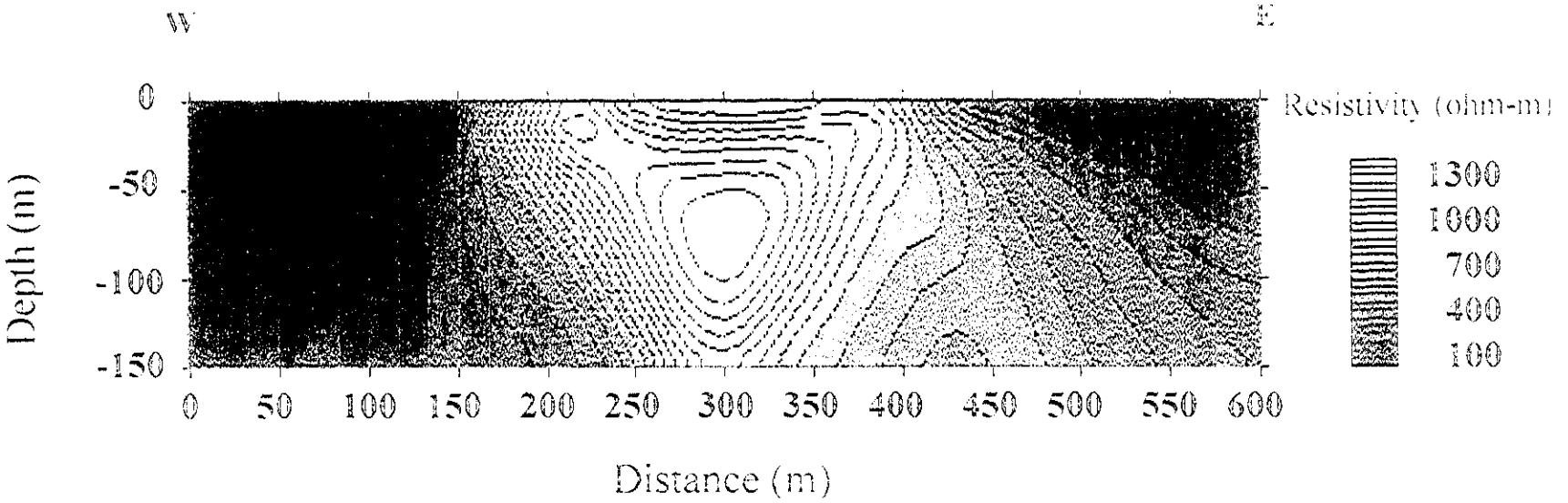

Figure 2.9 RIP result -Hóa Thương-

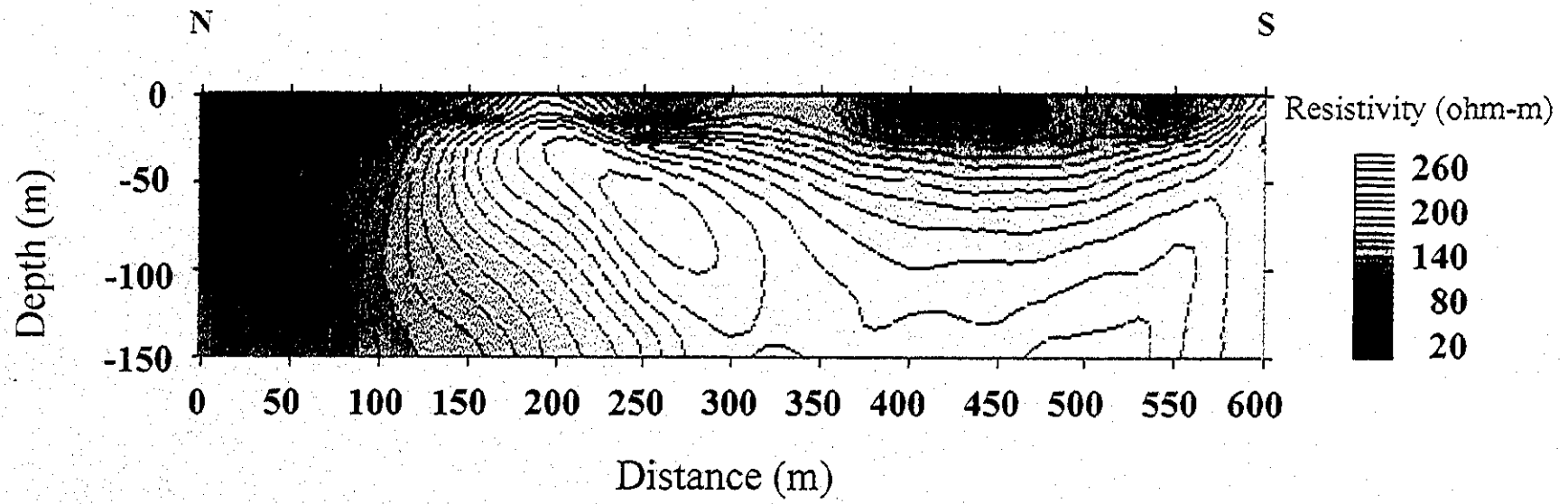

Figure 2.10 RIP Result Đồng Bẩm-

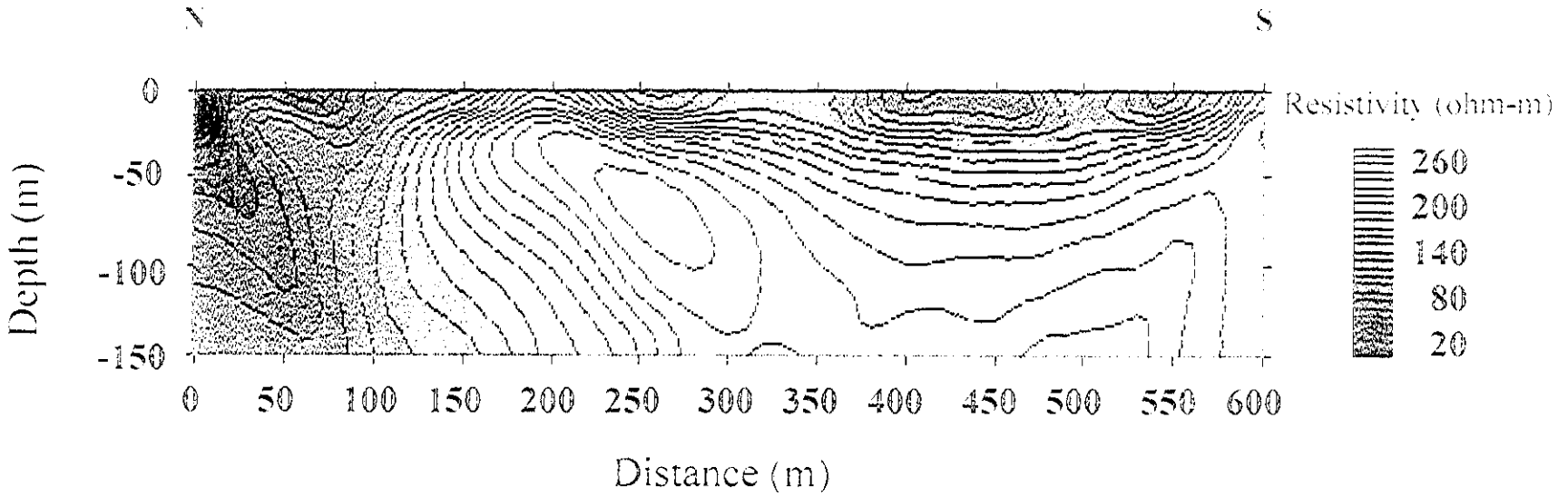

Figure 2.10 RIP Result Đồng Bẩm-

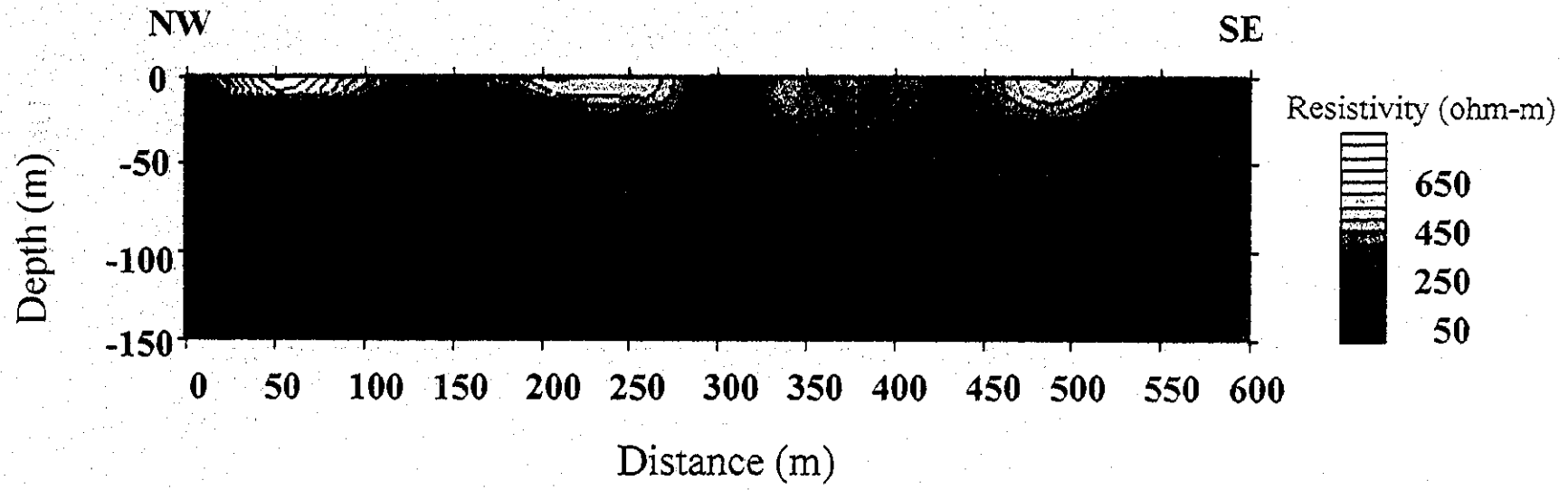

Figure 2.11 RIP Result -Thinh Dức-

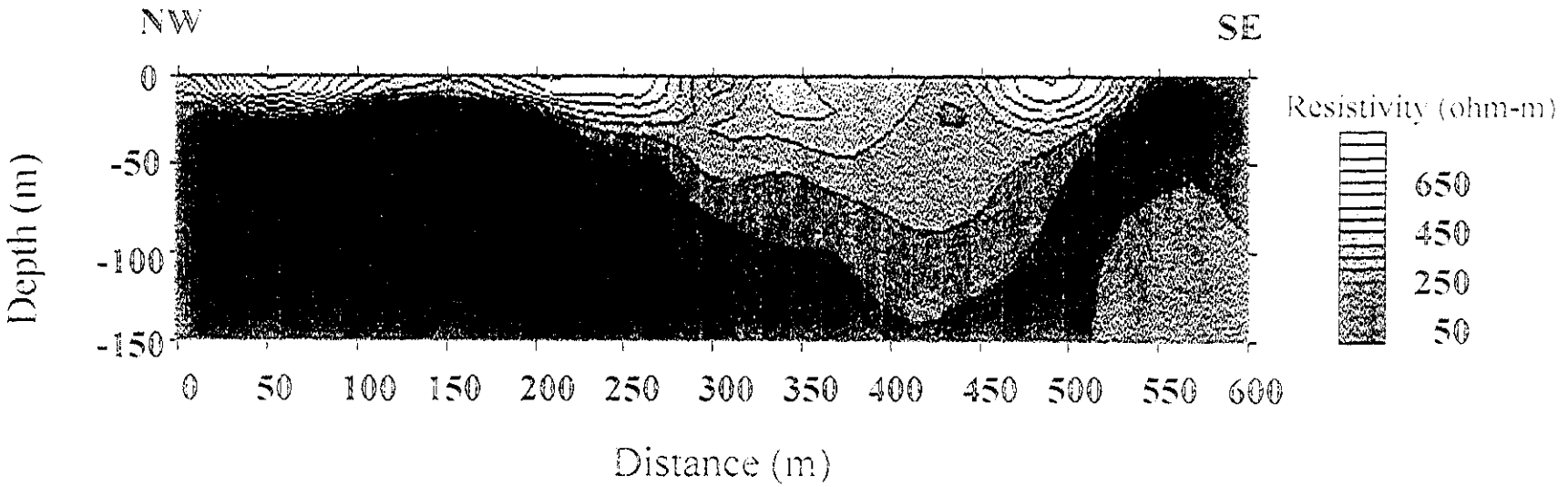

Figure 2.11 RIP Result -Thinh Dức-

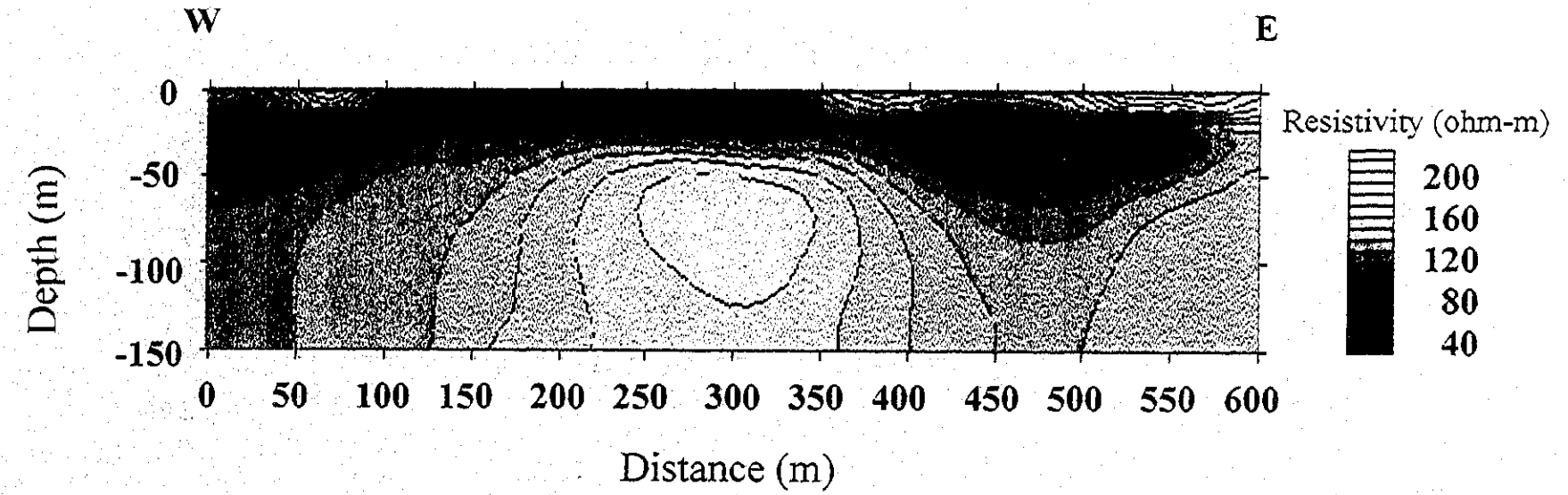

Figure 2.12 RIP Result -Nam Tiến-

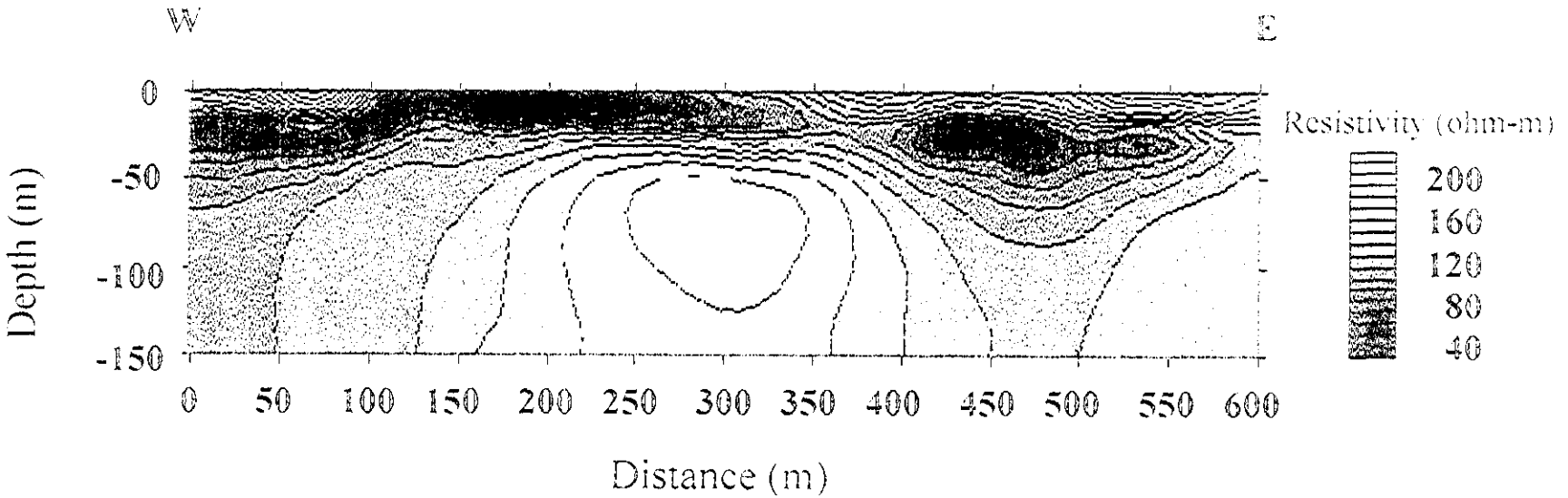

Figure 2.12 RIP Result -Nam Tiến-

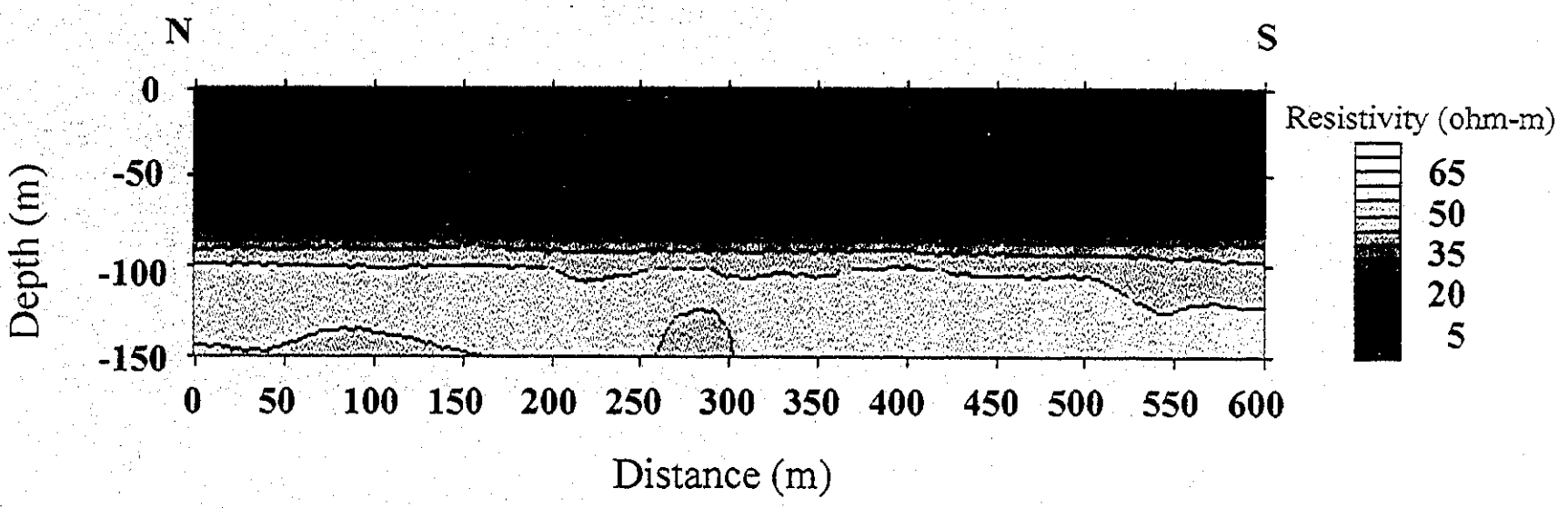

Figure 2.13 RIP Result -Yên Thăng-

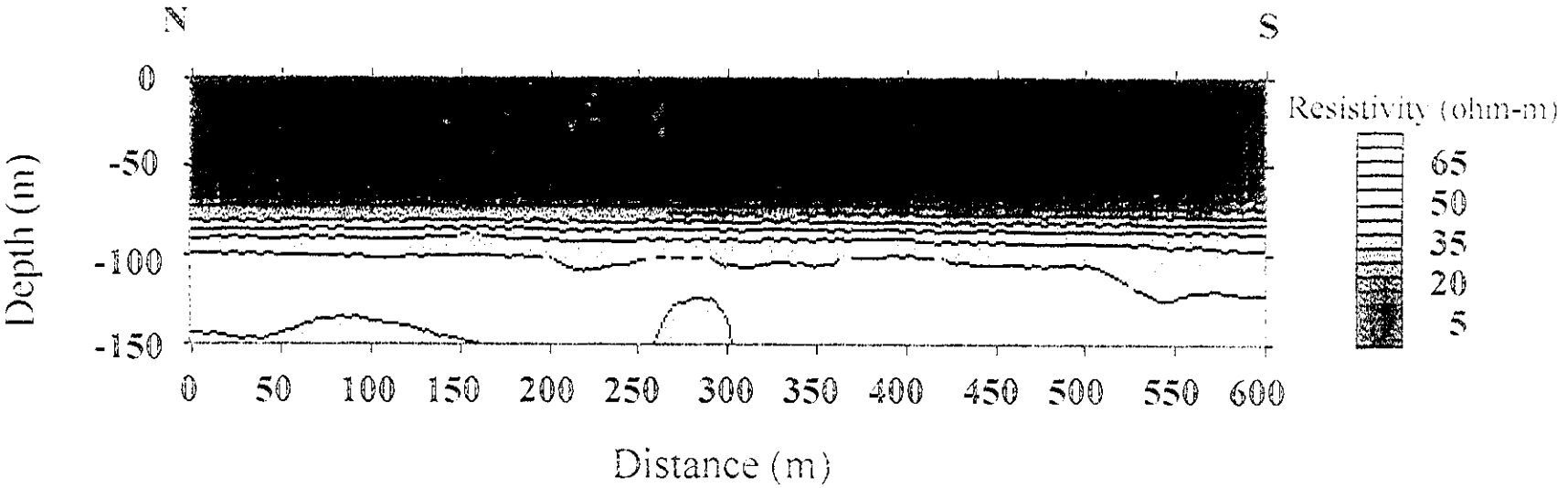

Figure 2.13 RIP Result -Yên Thăng-

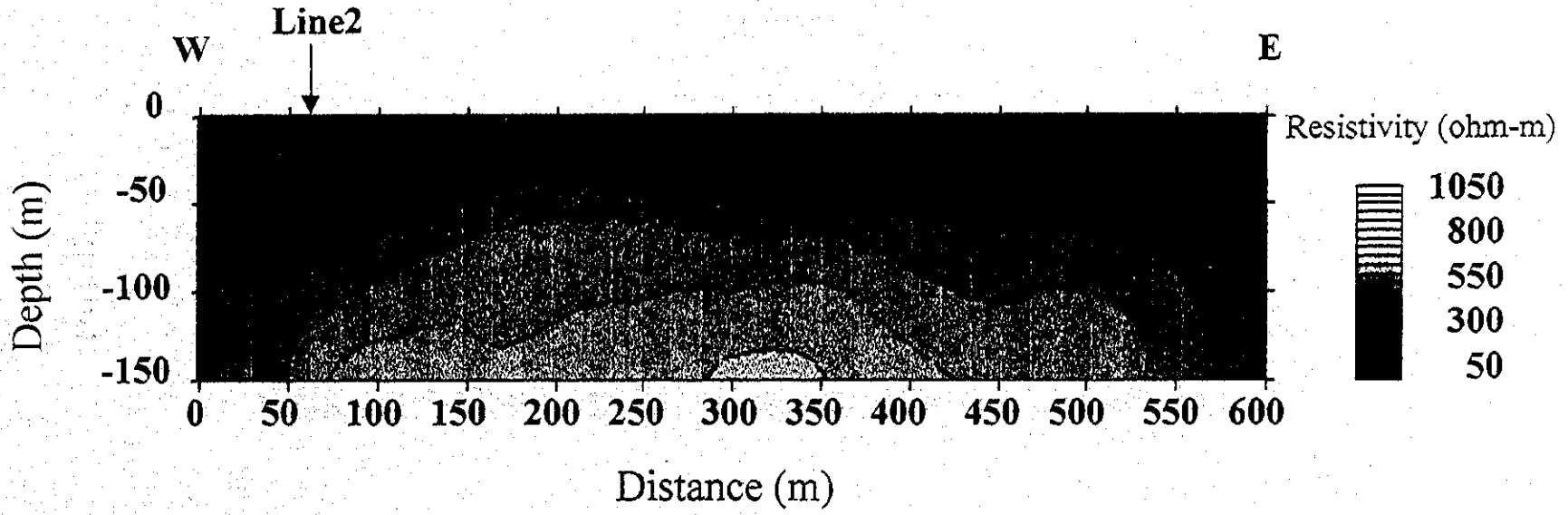

Figure 2.14 RIP Result - Quang Son(Line1) -

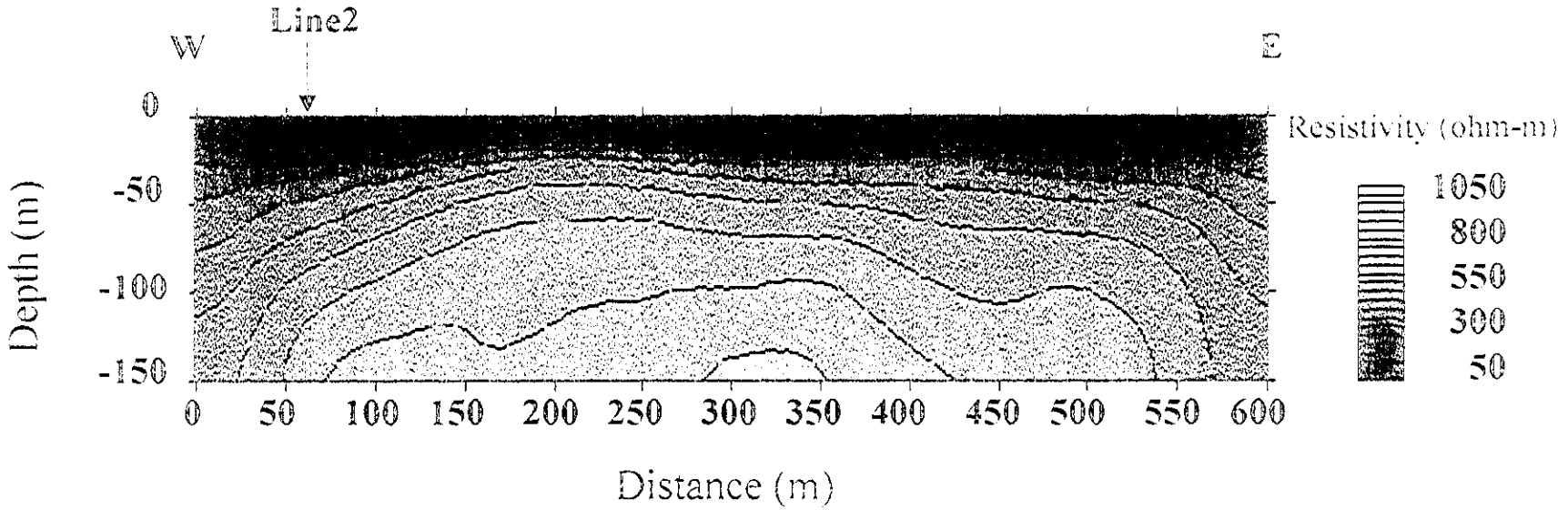

Figure 2.14 RIP Result - Quang Son(Line1) -

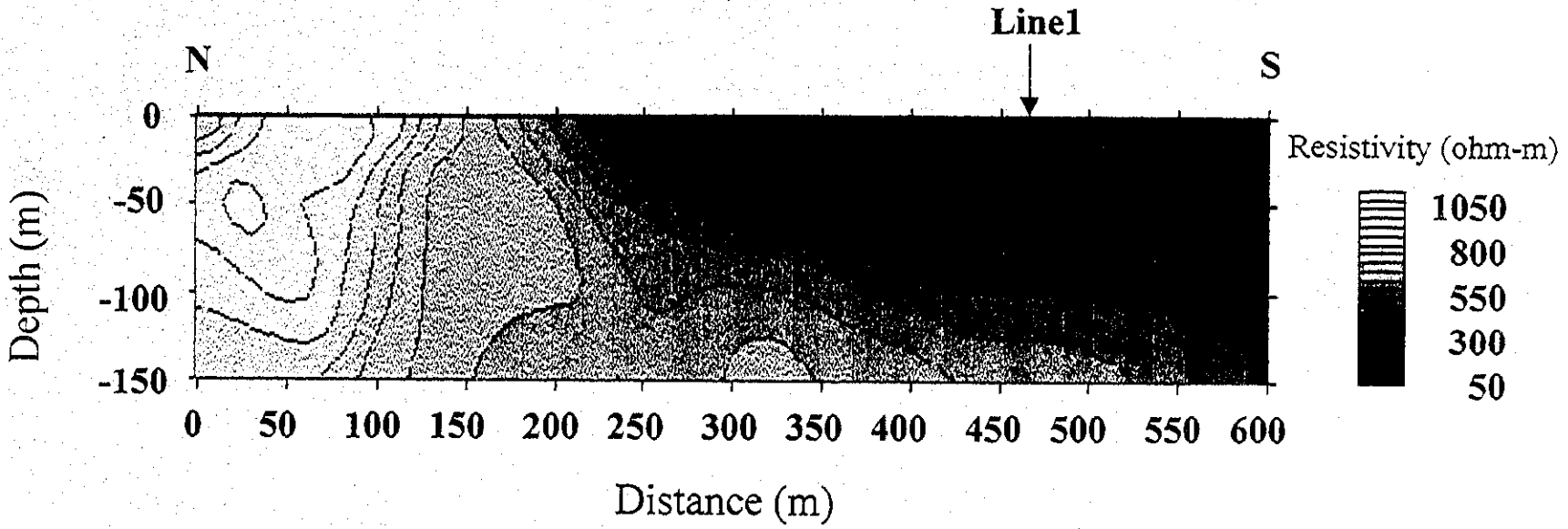

Figure 2.15 RIP Result - Quang Son(Line2) -

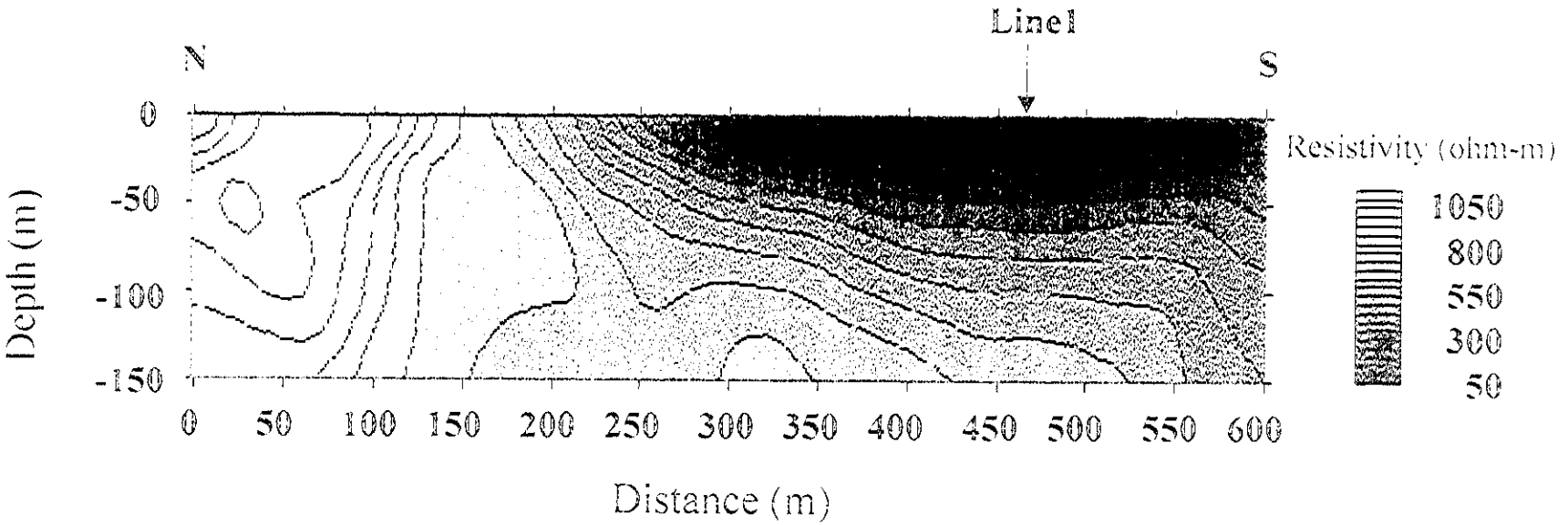

Figure 2.15 RIP Result - Quang Son(Line2) -

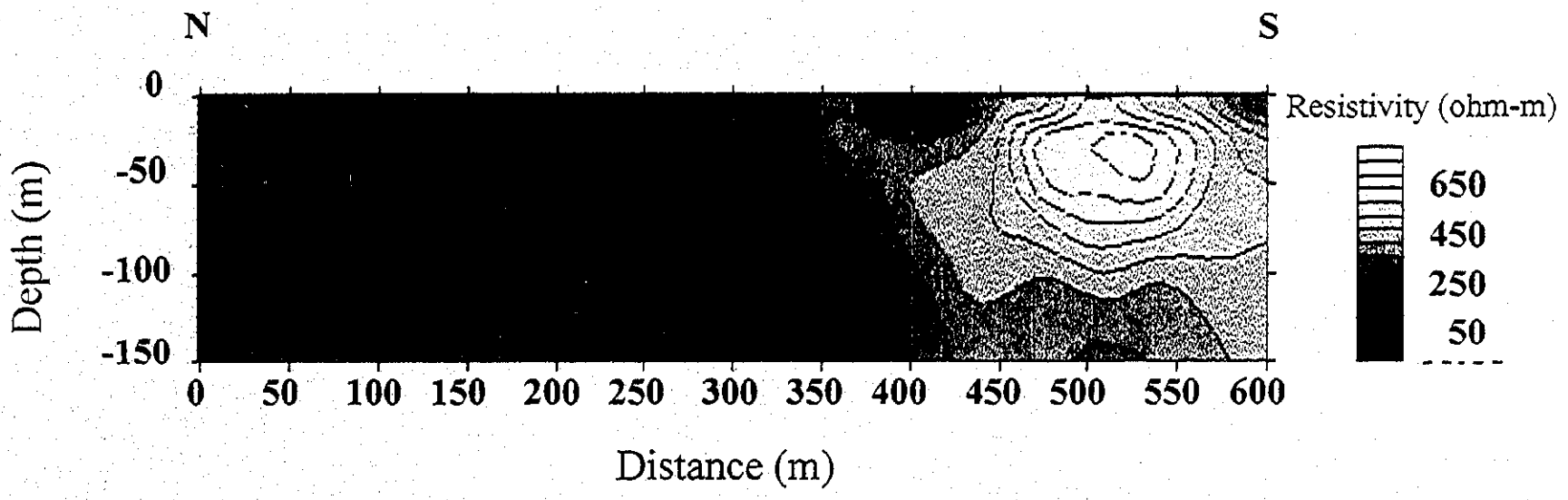

Figure 2.16 RIP Result -Đồng Phong-

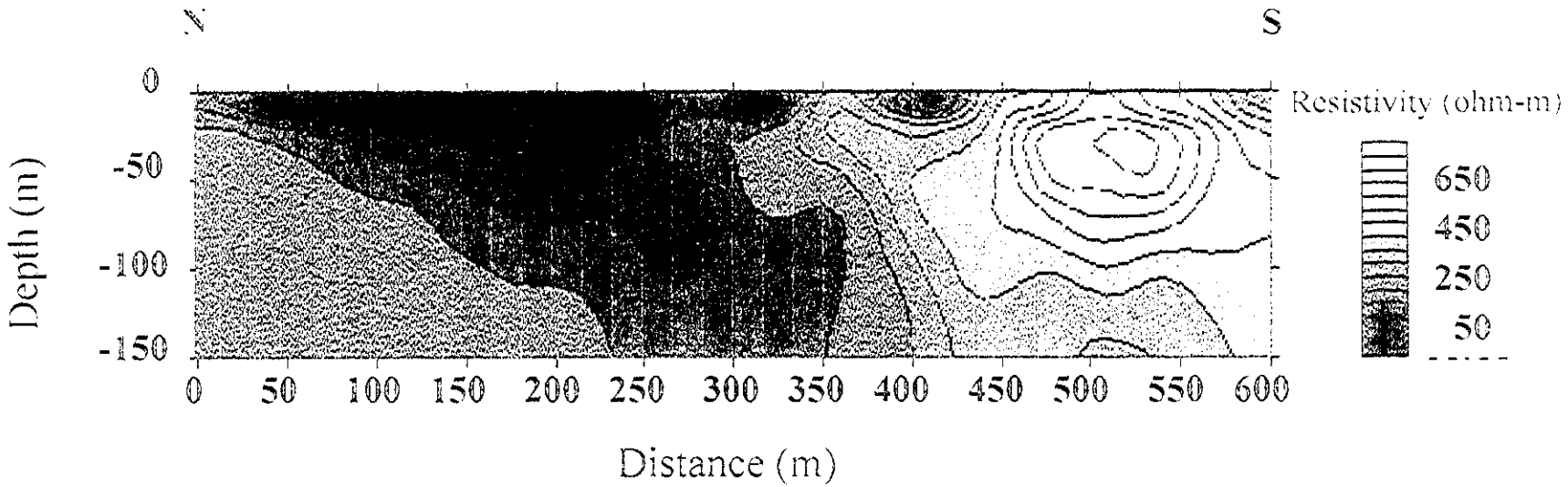

Figure 2.16 RIP Result -Đồng Phong-

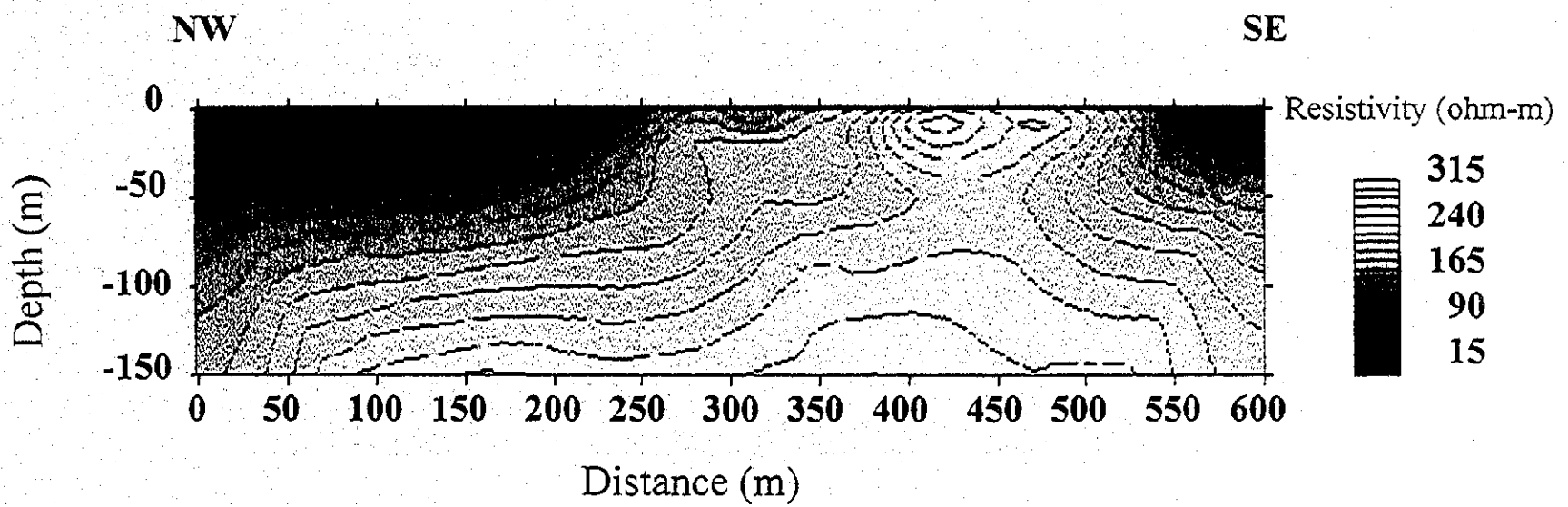

Figure 2.17 RIP Result -Vĩnh Thành-

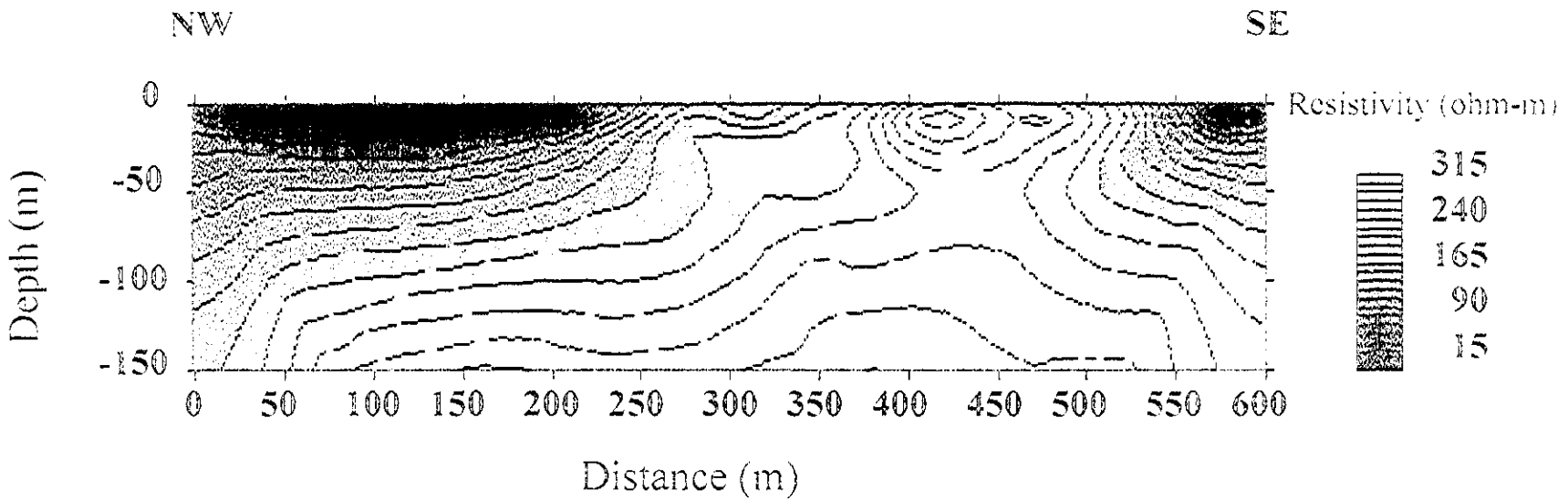

Figure 2.17 RIP Result -Vĩnh Thành-

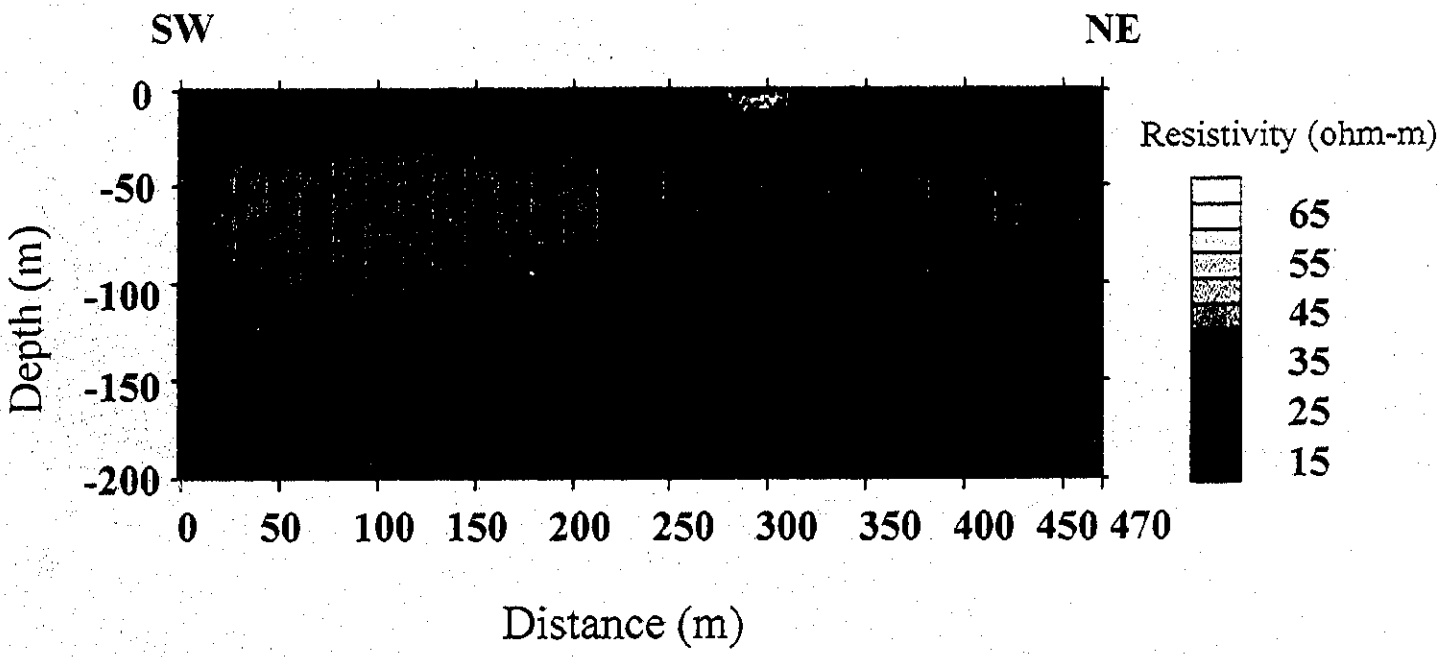

Figure 2.18 RIP Result -Đinh Tường-

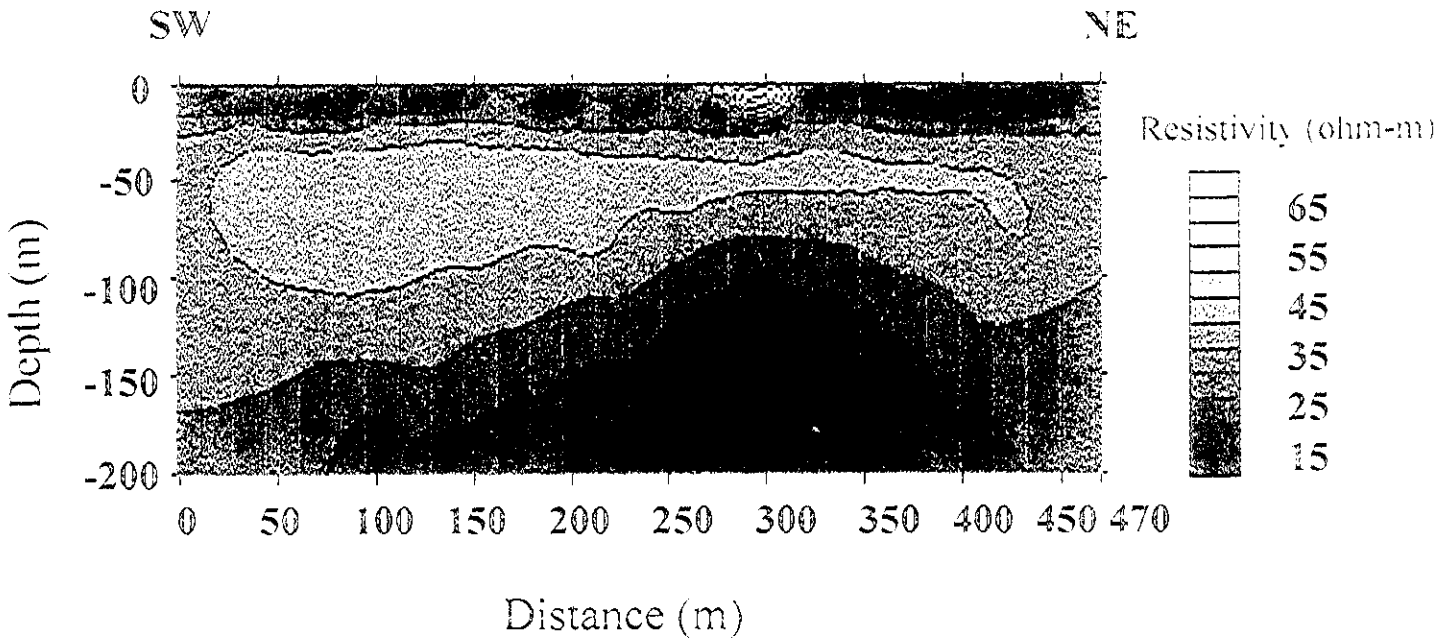

Figure 2.18 RIP Result -Đinh Tường-

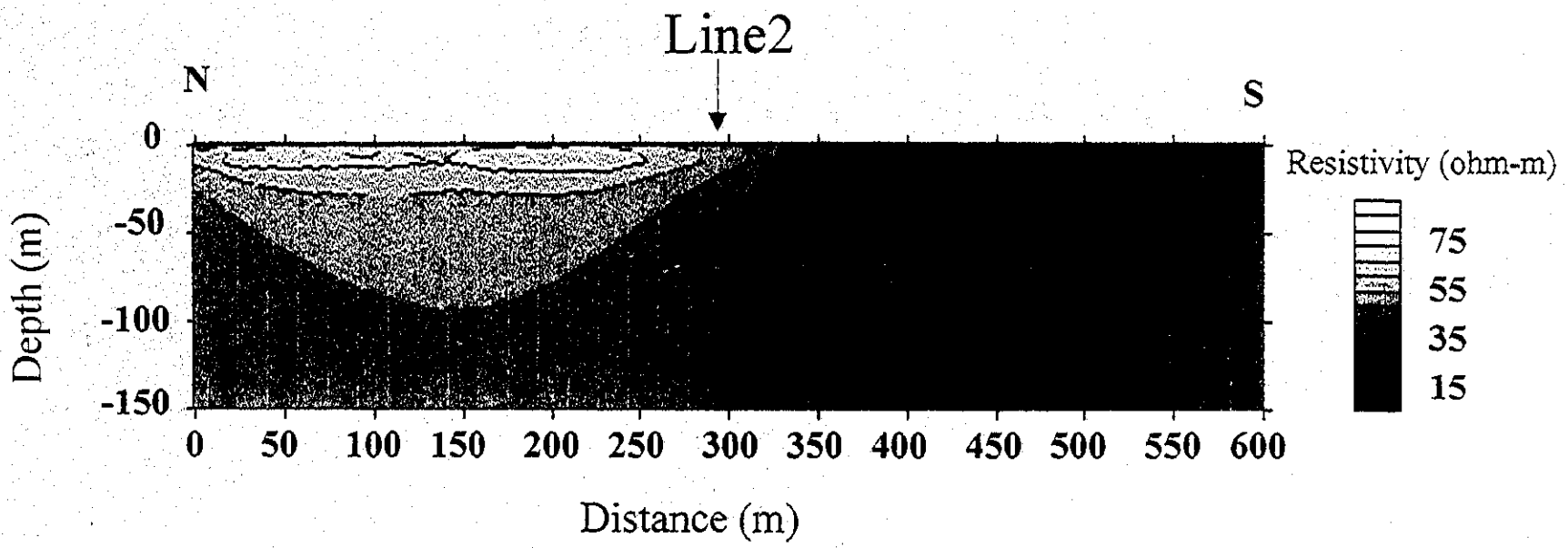

Figure 2.19 RIP Result -Thiêu Hưng(Line1)-

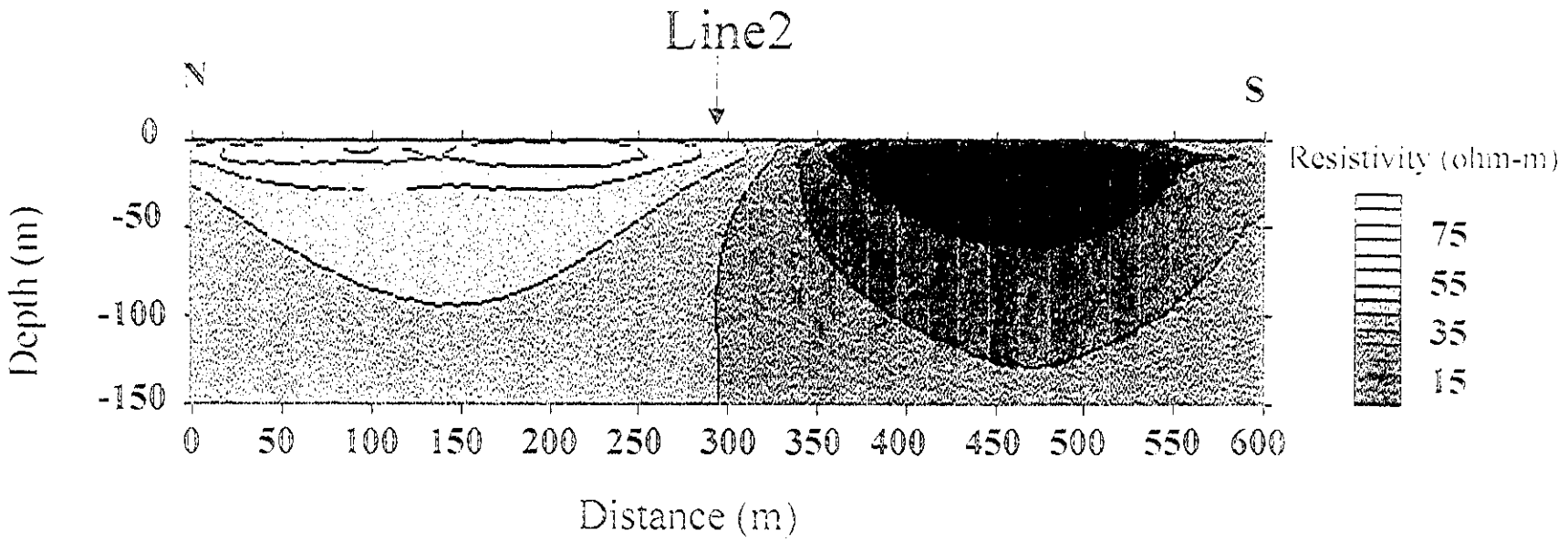

Figure 2.19 RIP Result -Thiêu Hưng(Line1)-

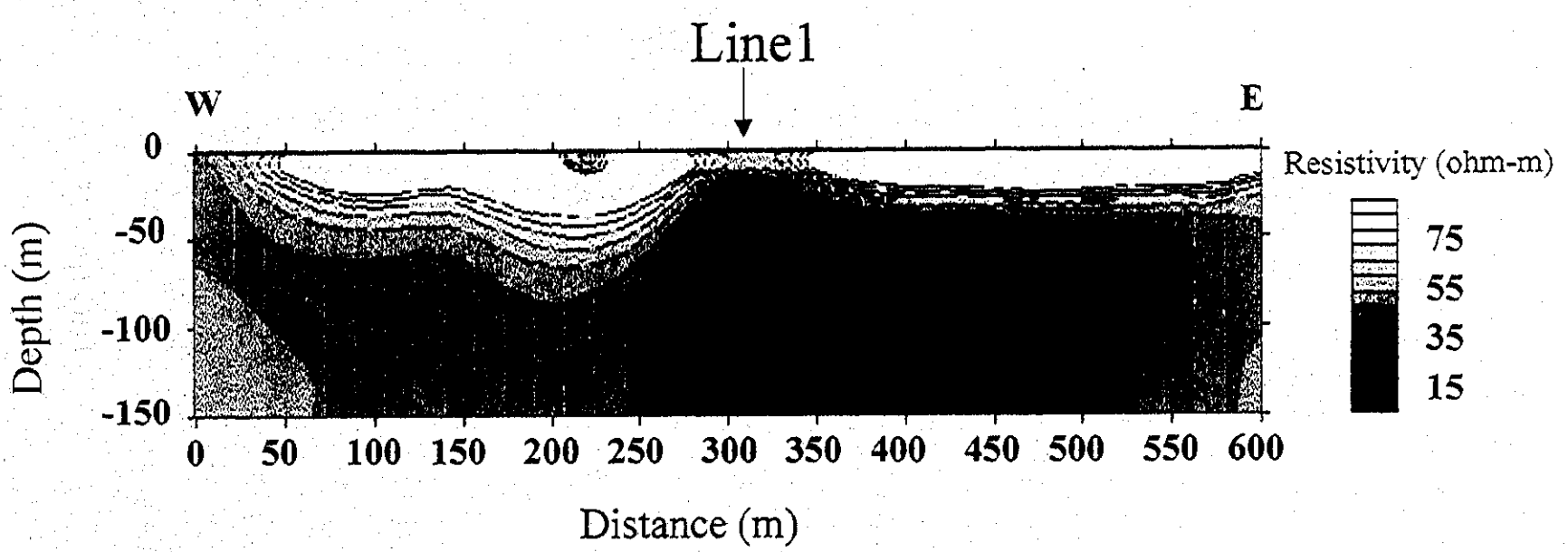

Figure 2.20 RIP Result -Thiêu Hưng (Line2)-

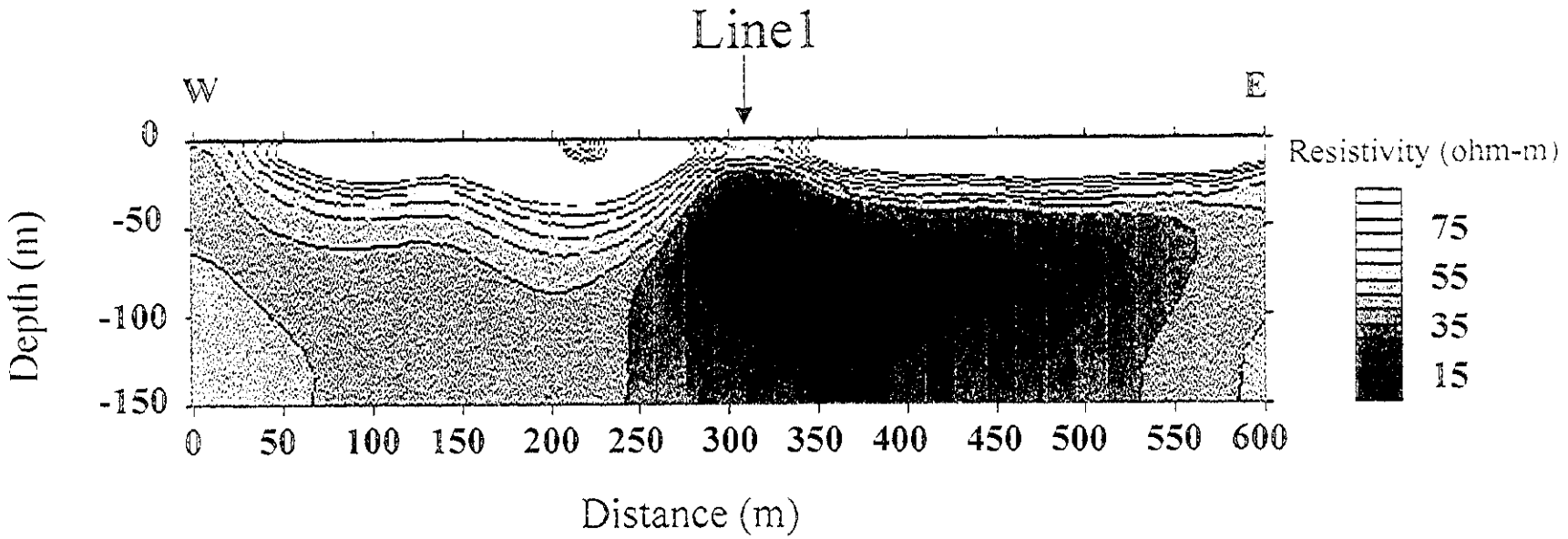

Figure 2.20 RIP Result -Thiêu Hưng (Line2)-

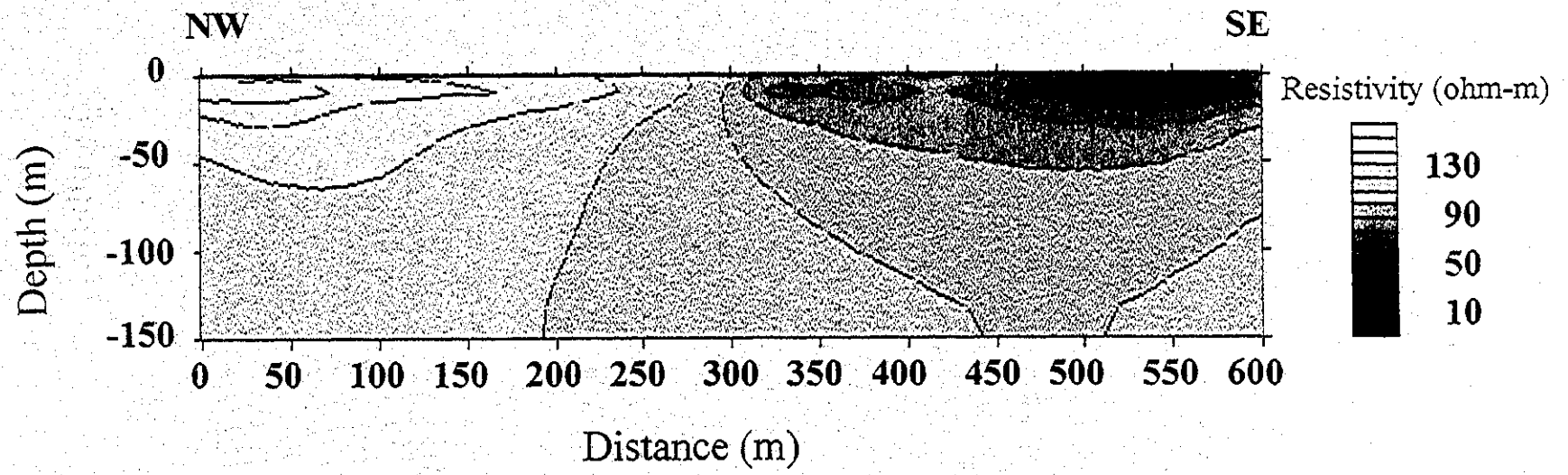

Figure 2.21 RIP Result -Van Thắng-

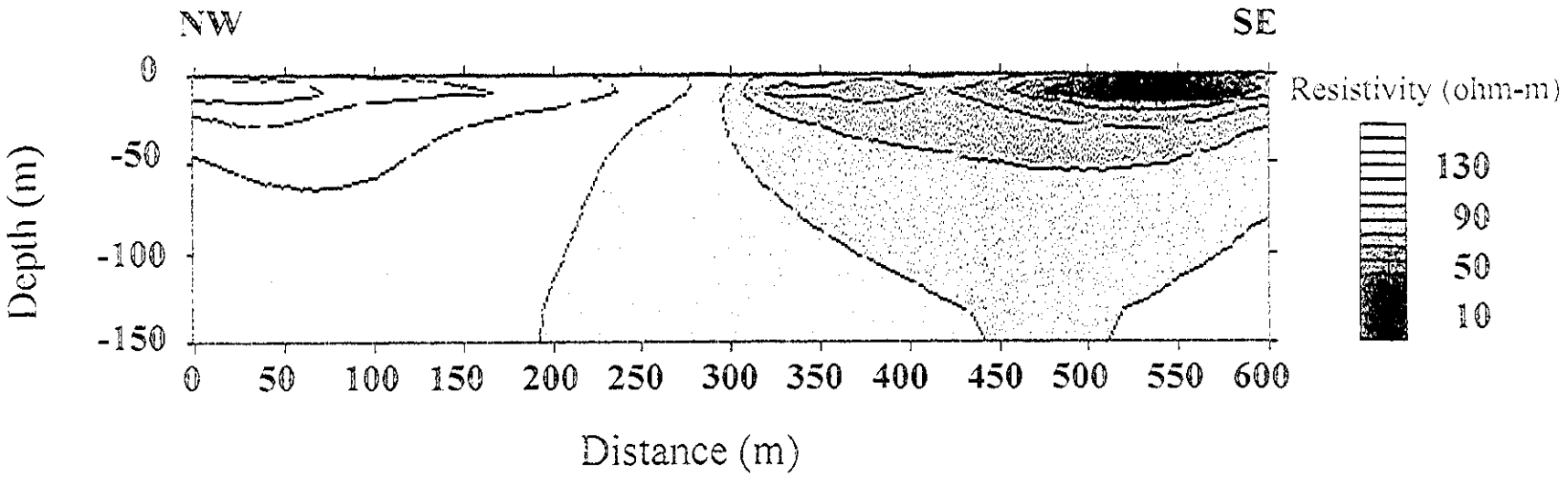

Figure 2.21 RIP Result -Van Thắng-

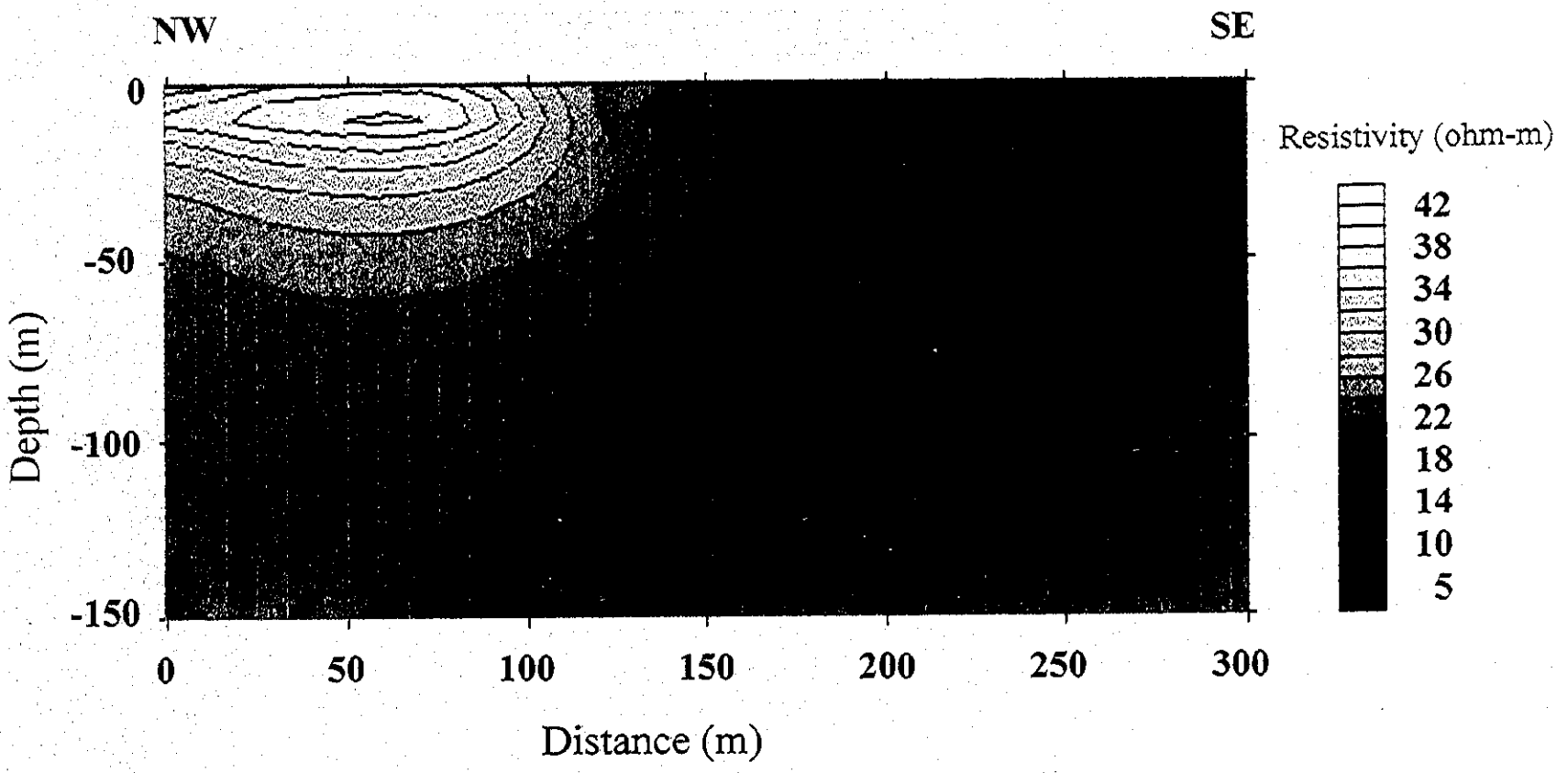

Figure 2.22 RIP Result - Đức Yên -

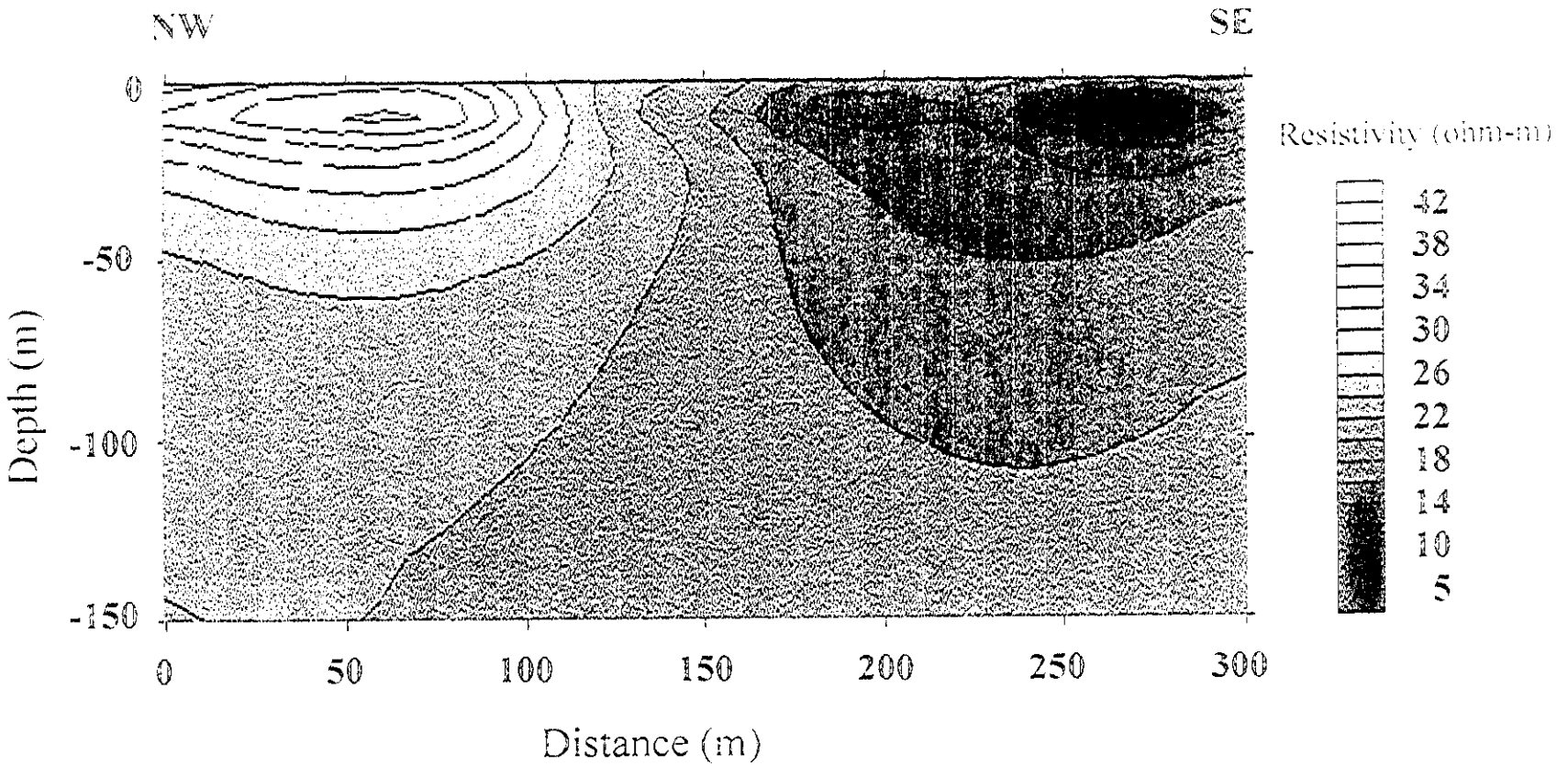

Figure 2.22 RIP Result - Đức Yên -

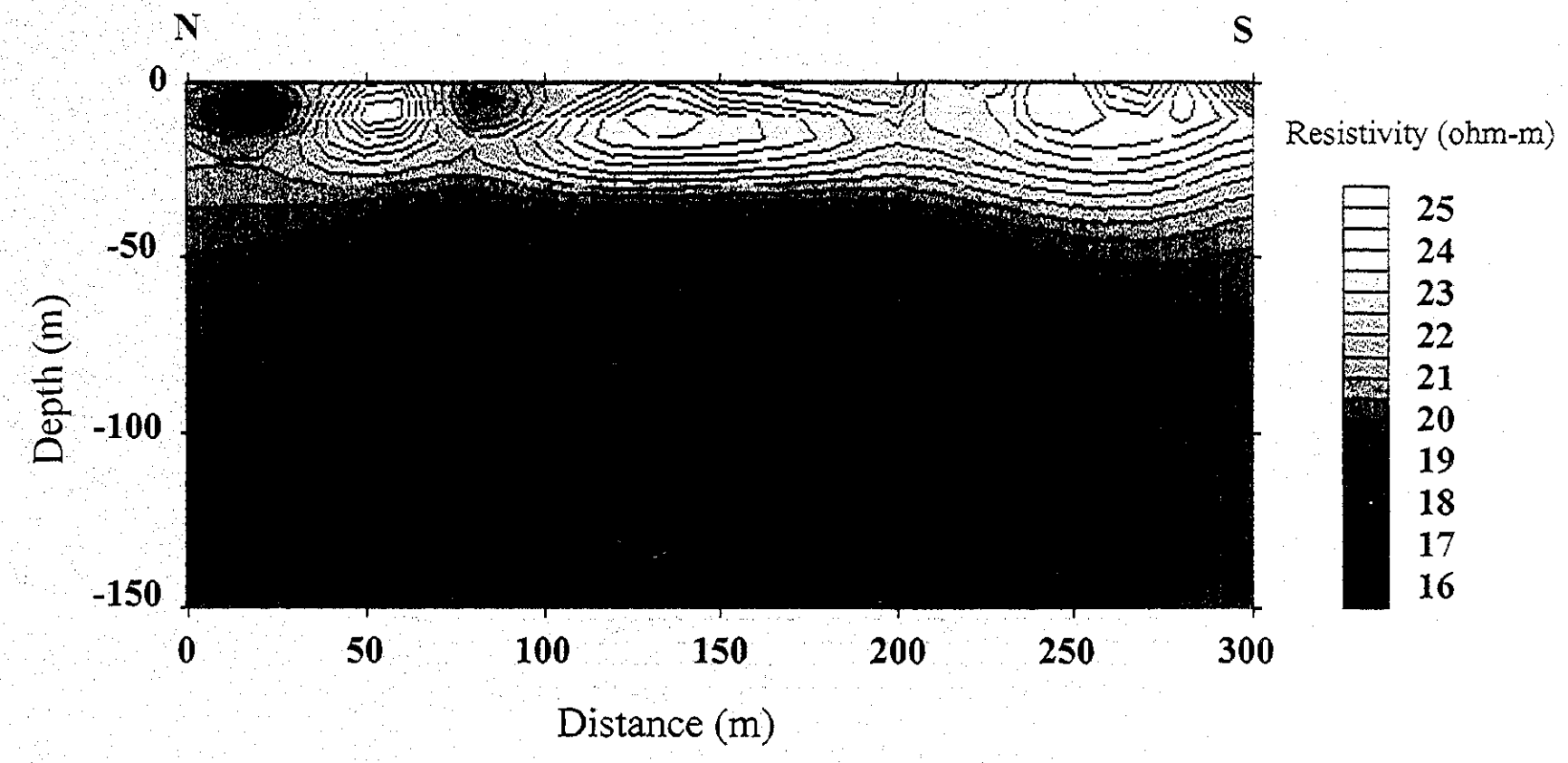

Figure 2.23 RIP Result - Trung Lễ -

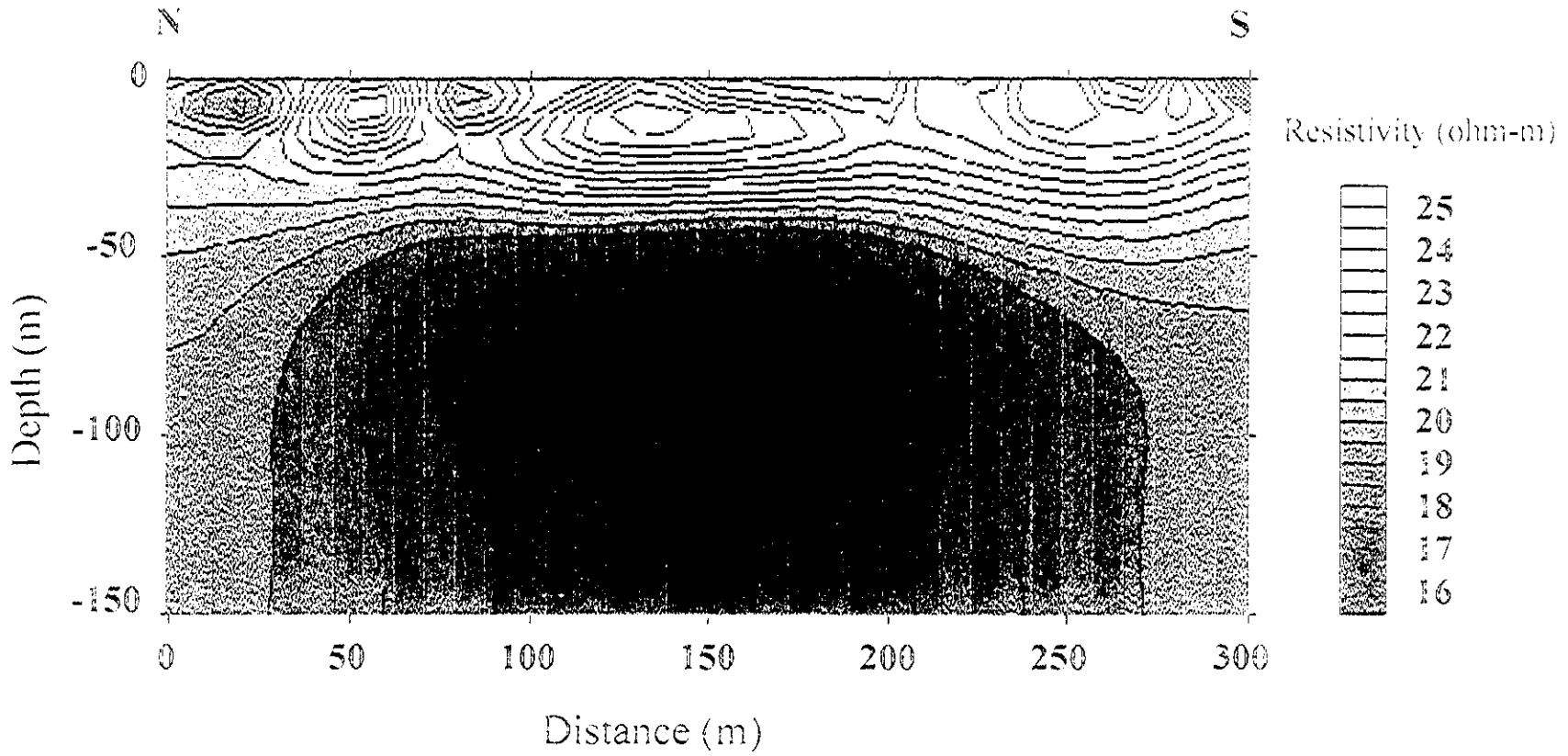

Figure 2.23 RIP Result - Trung Lễ -